IDENTIFYING THE MINERALOGY OF ROCK TEMPER IN CERAMICS USING X-RADIOGRAPHY

Christopher Carr and Jean-Christophe Komorowski

Industrial and medical x-radiography can be used in a manner analogous to back-scattered electron microscopy to identify the approximate mineralogy of rock temper particles in ceramics, but without their destruction by thin-sectioning, and at low cost. Particle traits similar to those used in petrography to identify a mineral are visible in a magnified x-radiograph. The traits include particle x-radiographic gray level, which varies with a particle's mean atomic number, specific gravity, and mineralogy; size; morphology; cleavage; and internal texture. Blind tests are made to evaluate the specificity and accuracy of the method. Its utility is shown through a study of the exchange of Ohio Middle Woodland ceramics.

La radiografía-x industrial y médica puede ser usadas en manera análoga a la microscopia electrónica de barrido, para identificar la mineralogía de las partículas de roca usadas como desgrasantes en la cerámica. Con este estudio las muestras de cerámica se destruyen minimamente ya que solo es necesario cortar una sección delgada, además de que el proceso se realiza a un bajo costo. Las características de las partículas similares a las usadas en la petrografía para identificar un mineral son visibles en una radiografía-x amplificada. Estos razgos incluyen el nivel gris de la partícula en la radiographía-x, que varía dependiendo de su número medio atómico, gravedad específica y mineralogía; tamaño; morfología; escisión; y textura interna. Se realizan "pruebas de ciego" para evaluar la especificidad y precisión del método. La utilidad se demuestra a través de un estudio del intercambio de cerámica en Ohio Middle Woodland.

The mineralogy of rock temper additives and natural inclusions in ceramics is an important aspect of material culture that archaeologists use to reconstruct the past. Differences in the mineralogy of aplastic particles have been used to identify vessels that differ in their engineering, function, date of manufacture, and source of manufacture (e.g., Bishop et al. 1982; Braun 1983; Freestone et al. 1982; Garrett 1986; Porter 1963; Shepard 1956; Stoltman 1989, 1991; Williams 1983). These kinds of information, in turn, speak directly to basic archaeological topics such as ceramic taxonomy, chronology, cultural affinity, social interaction and exchange, and settlement organization.

This article shows how x-radiography can be used in conjunction with traditional petrographic and other fine-scale methods in order to identify the mineralogy of rock aplastics in ceramics. It is the fourth of a series of articles (Carr 1990, 1993; Carr and Riddick 1990) that introduce and apply new ceramic x-radiographic methods. Here, we first define the relevant roles and general advantages of various traditional methods of mineral identification and x-radiographic methods relative to each other. The resolution level, sampling requirements, and costs of each method are considered. Second, procedures for applying x-radiography to the task of identifying aplastic mineralogy are introduced. The procedures are analogous in their physical basis to those of back-scattered electron microscopy. The theory behind and limitations to this analogy are discussed. Third, the results of two blind tests of the new x-radiographic method are presented. These compare x-radiographic to petrographic identifications of the mineralogy of rock aplastics. Specific potentials and limitations of the method are revealed. Finally, the utility of the method is briefly illustrated through a preliminary study of Ohio Middle Woodland utilitarian ceramics from the McGraw site (Prufer 1965) for their locations of

Christopher Carr ■ Department of Anthropology, Arizona State University, Tempe, AZ 85287-2401
Jean-Christophe Komorowski ■ Institute de Physique du Globe de Paris, 4 Place Jussieu, Tour 14-24, Boite 89, 75252 Paris Cedex 05, France

manufacture and possible exchange. The study suggests the nature of socioeconomic integration of Ohio Hopewell households.

The Role of X-Radiography Compared to Other Methods of Mineral Identification

In contemporary archaeology, the mineralogy of rock aplastics in ceramics can be identified with increasing specificity with a series of techniques. These include (1) the observation of aplastics exposed in freshly broken sherd edges by eye or with a hand lens of approximately 10× power; (2) low-power, approximately 20×, reflected-light, binocular microscopy of aplastics viewed on cut and/or polished sherd surfaces; and (3) high-power, petrographic microscopy of thin sections of sherds viewed under polarized light (Rye 1981:50–51; Shephard 1976:139–141, 157). Macroscopic and hand-lens observation allow broad, tentative identifications of common minerals based on crystal form, color, luster, and cleavage. Binocular microscopy can be used to verify and extend the list of mineral identifications using these same attributes. High-power petrography, which considers optical properties of minerals that vary with their microstructure (e.g., pleochroism, birefringence) and other subtle attributes (e.g., staining, abrasion, chemical weathering), allows subcategories of common minerals to be identified. Species of igneous and metamorphic rocks, sandstones, limestones, and sands varying in rare minerals can thus be distinguished (Shephard 1976:141).

Finer-scale methods not only allow mineral and rock identification with greater specificity, but also provide more exact estimates of the quantity and particle size distribution of aplastic particles of particular mineral and rock species. Observation by hand lens on broken sherd edges permits the viewer to distinguish the presence or absence and general size of particles of various minerals. Impressionistic, ordinal-scale estimates of the quantity and size of particles of various minerals are commonly made with low-power microscopic observation of cut sherds. Continuous-scale estimates of the fractional volume and size distribution of particles of various minerals and rock species can be made with petrographic methods (see Stoltman 1991 for a literature review).

Occasionally, petrographic mineral identifications have been supplemented with yet finer-grained chemical or structural characterizations provided by the electron microprobe (Yeatts 1990), scanning electron microscopy (Tite et al. 1982), back-scattered electron microscopy (Burton 1986; Simon 1988:204), instrumental neutron activation analysis (INAA) of aplastic separates (Elam et al. 1992), or X-ray diffraction (Bimson 1969; Isphording 1974; Simon 1988; Weymouth 1973). Back-scattered electron microscopy methods have also been used to simply survey particle mineralogy in a manner analogous to low-power microscopy, and to estimate mineral class fractional volumes in a manner analogous to petrography.

In studies of large ceramic assemblages, coarser methods are typically used first to survey and tentatively classify large numbers of sherds or vessels by their aplastic inclusions. Finer methods are used to verify the classification and provide precise mineralogical and petrological descriptions of the classes with a small sample of sherds.

A technique that uniquely combines surveying and descriptive capabilities between those of hand-lens and petrographic observation is x-radiography with a viewing magnification of 20× or more (Carr 1990; Carr and Riddick 1990). An x-radiograph of a pottery sherd reveals aplastic particles and any other internal phases or features that differ from each other in their composition, average specific gravity, and/or thickness and, thus, their transmittance of X-rays and their image gray level. (For example x-radiographs, see Carr 1990, 1992; Carr and Riddick 1990). Compared to other methods, x-radiography fills the following niche:

(1) X-radiography allows the identification of particle mineralogy with a precision between that of hand-lens observation and binocular microscopy.

(2) It permits the volume fraction and size distribution of particles of various minerals or families of minerals, or of all aplastics, to be estimated with a precision similar to or greater than petrography.

(3) At the same time, it can be used to survey large samples of sherds with a cost-effort similar

to that of binocular microscopic observation of cut sherds, and much less than that of petrography.

(4) X-radiography is a completely nondestructive technique, whereas the other methods require sherds to be broken, cut, or thin-sectioned.

The resolution of x-radiography in identifying the mineralogy of aplastics is evaluated in detail, below. As in binocular microscopic work, resolution depends on the degree of weathering and morphological distinction of crystals. Common minerals and mineral families that we have distinguished in our work with Ohio ceramics include quartz; k-feldspar; other feldspars; biotite; other micas; sericite; pyroxene, amphiboles, or pyriboles more generally; epidotes and sphenes; other mafic minerals; and opaque oxides and sulfides.

In estimating the fractional volume and size distribution of aplastic particles of identifiable minerals or mineral families, x-radiography has an advantage over hand-lens, binocular, and petrographic methods. It allows a larger sample volume of a sherd or vessel to be studied and quantified. The entire volume of a sherd or large areas of a whole vessel can be imaged in an x-radiograph. In contrast, a typical petrographic thin section is less than 5 cm long, as wide as the vessel's wall, and only 30 μ thick. Our experience has shown that the aplastic particles contained in this small volume need not accurately represent the fractional volume and size distribution of all particles or of particles of particular minerals within a vessel, if the inclusions are coarse and mineralogically heterogeneous. Ohio Woodland ceramics tempered with crushed rocks derived from glacial tills are cases in point (Carr 1993:99–100). Multiple thin sections cut from different parts of a vessel may be required to assess accurately the fractional volume and size distribution of all particles or particles of specific minerals within the vessel. Given cost limitations, however, this solution is a trade-off, augmenting sample size problems at the assemblage level, and is rarely used.

X-radiography allows the survey and description of large numbers of sherds or vessels from an assemblage because its cost is modest. Producing an x-radiograph of a sherd or vessel section requires about \$.13 in labor and materials on the average. This estimate is based on the radiographing of more than 3,500 Ohio Woodland sherds

and vessels (Carr and Riddick 1990:62). The low cost derives in part from the capability of radiographing multiple sherds on a single sheet of film. In contrast, a single petrographic thin section used in petrographic and electron microscopy currently costs about 6 to 18 American dollars in labor and supplies to prepare. The cost in time to identify the mineralogy of aplastics imaged in an x-radiograph is similar to that in binocular microscopic work.

The resolution and cost of x-radiography give it a unique niche in ceramic archaeology compared to other methods for identifying the mineralogy of aplastics. X-radiography can be used to study large samples of sherds, each sherd in some detail. In contrast, when hand-lens observation and binocular and petrographic microscopy are combined in the traditional, multilevel research design described above, large samples of sherds can be surveyed but only a small number can be described in detail. This approach can lead to certain classes of ceramics not being identified or discriminated in a collection. The approach can also prohibit the estimation of the relative frequencies of certain classes and allow only their occurrence in the collection to be documented. Cases in point include rare classes; classes defined by rare, identifiable minerals; and classes distinguished by only the proportions, rather than the occurrence, of certain minerals.

For example, in a ceramic assemblage, it might not be possible with hand-lens and binocular microscopic information to identify trade and local wares that differ moderately in the fractional volumes of their mineral inclusions. Ceramics tempered with heterogeneous glacial tills can pose this problem. At the same time, petrographic microscopy on a small sample from the assemblage might allow only the presence of trade wares, not their relative frequencies, to be determined, and rarer trade wares might not be represented at all in the sample. In this situation, behavioral reconstructions of exchange would be restricted, at best, to a qualitative rather than quantitative scale. Yet having quantitative estimates of exchange is essential to modeling the continuous-scale dynamics and structure of a cultural system, which lie at the heart of its stability or evolution (e.g., Braun 1987; Plog 1974). In this

Table 1. Optimal X-Radiographic Methods for Documenting the Mineralogy of Aplastic Particles in Ceramics.

1. Industrial films (e.g., Kodak Industrex M, R) or mammography films (e.g., Kodak Ortho M) that provide high-image contrast and a fine enough grain for their inspection under a magnification of more than 20×.
2. X-ray tube with a molybdenum rather than tungsten target, to maximize image contrast.
3. Low tube peak kilovoltages (ca. 20–50 KvP), just barely sufficient for passing through the specimen, to maximize image contrast.
4. X-ray housing with a beryllium window, to maximize image contrast.
5. No use of diaphrams or filters, to maximize image contrast.
6. Use of only back lead screens, to maximize image contrast.
7. Exposure of film with a somewhat dark balance.
8. Use of a strong incandescent light source for examining a film.
9. X-ray tube with small focal spot (< ca. .7 mm), to maximize image clarity and allow image inspection under magnification.
10. Large focal spot-to-film distances (> ca. 30 in.), to maximize image clarity.
11. Specimen-to-film distance as small as curvature of vessel and film positioning allow (essentially 0), to maximize image clarity.

situation, x-radiography would be a more appropriate methodology.

In sum, x-radiography has potential for filling a niche in ceramic analysis not fully met by hand-lens observation, low-power binocular microscopy, and high-power petrographic microscopy used alone or together. Its levels of resolution of particle mineralogy, size, and fractional volume, along with its modest costs and nondestructive nature, make it appropriate for describing large samples of sherds in moderate detail.

Procedures for Identifying the Mineralogy of Rock Aplastics with X-Radiography

The procedures that allow the mineralogy of rock aplastics to be identified with x-radiography are of two kinds. First is the laboratory procedures for making x-radiographs. Only some carefully selected x-radiographic materials and equipment are effective for documenting rock aplastics. This is so because some rock aplastics differ from their clay matrices and from each other only slightly in their elemental composition and specific gravity. Thus, the relative degrees to which they absorb x-

rays and have the potential for creating images that differ in gray level from each other and from the clay can be slight. This problem can be minimized by using the industrial and medical x-radiographic procedures specified in Table 1 and by Carr and Riddick (1990).

The second kind of procedures that is required to determine the mineralogy of rock aplastics is the logical rules and operational criteria for identifying particular inclusions to their mineralogical species or families. These procedures involve three topics: (1) the x-radiographically determinable traits of aplastic particles that can be used for identification, (2) an analogy between the x-radiographic trait of particle image gray level and the back-scattered electron microscopy trait of particle image brightness, and (3) the taxonomic key of rules by which particle traits are combined to identify their mineralogy. Each of these topics is discussed in turn.

Particle Traits

An x-radiograph of the rock aplastics within a sherd registers many of the same kinds of characteristics that are used in petrography to identify their mineralogy. These are summarized in Table 2. In petrography, both morphological and microstructural–optical characteristics of a crystal are essential to identifying its mineral species. Most of the morphological characteristics used are also observable in the x-radiographic image of a crystal, save the presence, number, and angle of internal crystal cleavage planes it has. In an x-radiograph, only the presence, number, and angle of external crystal faces are observable. Crystal faces are less useful than crystal cleavage planes for mineral identification because the faces may have been weathered away. Also, many mineral species have similar types of faces.

None of the microstructural–optical characteristics of rock aplastics that are often observable petrographically are directly recorded in an x-radiograph. However, analogous traits are useful. In place of the color and opaqueness of a crystal, its x-radiographic gray level can be observed. In place of the pleochroism, birefringence, and spatial pattern of birefringence of a crystal, its internal texture can sometimes be seen. In general, the x-radiographically determinable, structural–opti-

Table 2. Characteristics of Aplastic Particles in Ceramics Used in Petrography to Identify Their Mineralogy and Corresponding Traits Observable with X-Radiography.

Petrography	X-Radiography
Mophological traits	
Crystal outline shape: equant, oblate, prolate, angular, subangular, rounded, etc.	observable
Crystal form: euhedral, subhedral, anhedral	observable
Crystal size	observable
Presence, number, and angle of crystal cleavage planes	presence, number, and angle of only crystal faces
Relief	no corresponding trait
Microstructural, optical traits	
Color, opaqueness	gray level
Pleochroism[a]	particle internal texture (a macrostructural, approximately equivalent trait)
Indicatrix form[b]	particle internal texture (a macrostructural, approximately equivalent trait)
Birefringence[c]	particle internal texture (a macrostructural, approximately equivalent trait)
Spatial pattern of birefringence: twinning, polysynthetic twinning, etc.	particle internal texture (a macrostructural, approximately equivalent trait)
Angle of extinction[d]	no corresponding trait

[a]Pleochroism is the expression of different colors by a crystal when visible light is transmitted through it in different directions. It results from the selective absorption of light of certain wavelengths in certain directions in minerals that have an anisotropic crystal structure.

[b]Indicatrix form describes a crystal's refractive indexes, which determine the velocity of refracted light rays along the crystal's various axes. Minerals may be isotropic, uniaxial, or biaxial, depending on the equality or inequality of their refractive indexes in different directions.

[c]Birefringence is the difference between the least and greatest refractive indexes of an anisotropic crystal, which is expressed as interference colors. Lighter colors indicate a higher birefringence.

[d]Extinction occurs when a doubly refracting crystal lets no light through in crossed polarized illumination. The angle of extinction is measured between a crystal's cleavage line or boundary and the nearest position of extinction as the microscope stage is rotated.

[e]The internal texture of a crystal is the geometric relationships among clevage planes, fractures, twinning planes, crystal intergrowths, etc., which lead to its overall visual appearance as homogeneous, foliated, fibrous, granular, etc.

cal characteristics of crystals are less precise indicators of mineralogy than the petrographically determinable traits to which they are analogous.

In sum, an x-radiograph provides much information that is essential to identifying the mineralogy of rock aplastics in ceramics, although less and different information than a petrographic thin section. Thus, the level of specificity and confidence with which mineral identifications can be made with an x-radiograph remains to be determined, both theoretically and empirically.

Analogy between X-Radiographic Image Gray Level and Back-Scattered Electron Microscopy Image Gray Level

Of the several kinds of particle traits that can be seen in an x-radiograph and that are useful for identifying its mineralogy, image gray level has the least obvious relationship to mineralogy. This relationship was explored theoretically in order to develop systematic rules for equating image gray level to particle mineralogy. We later evaluate the rules empirically.

When a standardized x-radiographic procedure is used to study a ceramic sherd (e.g., Carr and Riddick 1990), the image gray level of any particle of set thickness relative to the image gray level of some material standard of a set thickness depends on two factors. First is the mean of the atomic numbers of the elements that make up the crystal, weighted according to their proportions. Second is the particle's specific gravity. Both factors affect the proportion of incident X-rays that are absorbed by the particle versus those that are

Figure 1. X-radiographic image gray level (density) increases systematically with the mean atomic number of the studied medium when a standardized x-radiographic procedure is used. Here, the image gray level of the medium is measured relative to that of steel and aluminum standards, at the set peak kilovoltages of 100 and 200 KvP, respectively. In ceramic research, particle image gray level is measured relative to that of clay as a standard, and at some set peak kilovoltage between 20 and 50 KvP.
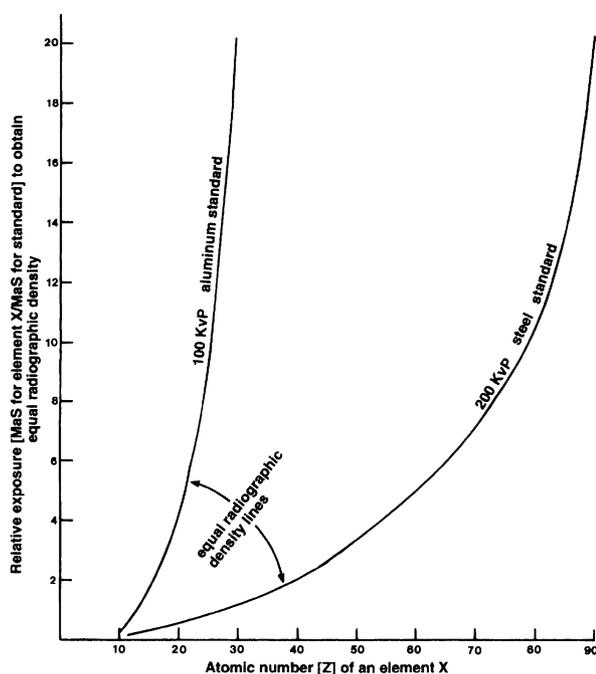
transmitted and expose the film. Because different minerals are comprised of different elements in different proportions, they have different mean atomic numbers and specific gravities. Thus, they create x-radiographic images that tend to differ in gray level relative to a material standard and relative to each other when the laboratory procedures, the thickness of the particles, and the standard's thickness are each held constant. In ceramic research, for this to be strictly the case, the particles must be similar in size, shape, and/or orientation, and sherds must be similar in thickness.

Of the two factors, mean atomic number and specific gravity, the former usually exerts a much greater effect than the latter on the image gray level of a particle. For example, lead has a specific gravity approximately 1.5 times that of ordinary steel. Yet 2.6 mm of lead produce the same relative exposure as 12 times that thickness (30.7 mm) of steel at 220 KvP (Eastman Kodak 1980). This reflects the high atomic number of lead. Thus, the image gray level of a particle relative to some standard becomes, to a large degree, a curvilinear function of the mean atomic number of the particle's constituent elements. This kind of relationship is well established in industrial x-radiography. For example, Figure 1 shows that the image gray level of a specimen comprised of a given element and having a set thickness increases regularly with the element's atomic number, when gray level is measured relative to that of an aluminum or steel standard of a set thickness.

The x-radiographic image gray level of a specimen is a relative measure. It can be assessed meaningfully only relative to the image gray level of some standard. An aluminum, steel, or lead sheet of set, appropriate thickness can be radiographed with sherds to provide this standard. We call this measure of a specimen its "x-radiographic relative gray level" (XRGL).

A more approximate, but more convenient "standard" than a metal sheet for qualitatively assessing a particle's XRGL is the adjacent paste matrix. Commonly, the paste will also be an acceptable standard if it is primarily clay and sparse in powdered rock additives or natural silts that vary in mineralogy.[1] This is so because the clays selected to make vessels within one site or several sites in a region typically will vary little in their mean atomic number and specific gravity compared to the range of mean atomic numbers and specific gravities of the minerals composing the vessels' aplastics, and compared to the sensitivity of radiographic films. On a worldwide

Table 3. Discriminating Characteristics of Some Common Rock-Forming Minerals.

Mineral	Chemical Formulae	Mean Atomic Number	Specific Gravity	Outline Shape	Crystal Form	Crystal Cleavage Planes
Clays			1.8 – 2.6	n.a.	n.a.	
Kaolinite	$Al_4Si_4O_{10}(OH)_8$	7.25	2.60 – 2.63	n.a	n.a.	
Chlorite	$Mg_6Si_6Al_2O_{20}(OH)_4Mg_6(OH)_{12}$	7.75		n.a.	n.a.	1 perfect
Montmorillonite (without inter-crystal water, Mg)	$Al_{3.5}Mg_5Si_8O_{20}(OH)_4$	9.101		n.a.	n.a.	
Illite	$Al_4Si_7Al\ O_{20}(OH)_4K_{.8}$	9.355		n.a.	n.a.	
Vermiculite	$Mg_6Si_7Al\ O_{20}(OH)_4(xH_2O,Mg)$	10.528		n.a.	n.a.	
Felsic minerals						
Chalcedony	SiO_2	10.000	2.55 – 2.63	crystalline		none
Quartz	SiO_2	10.000	2.59 – 2.66	o,p,e	eu,s,a	none
K-feldspar (orthoclase sanidine)	$K_2O.Al_2O_3.6SiO_2$	10.615	2.56	o,p,e	eu,s,a	1 good, 1 perfect at 90°
Na-feldspar (albite)	$Na_2O.Al_2O_3.6SiO_2$	10.000	2.61 – 2.64	o,p,e	eu,s,a	2 good, at 86°
Ca-feldspar (anorthite)	$CaO.Al_2O_3.2SiO_2$	9.923	2.703 – 2.763	o,p,e	eu,s,a	2 good, at 86°
Calcite	$CaCO_3$	10.000	2.711	e,o	eu,s	3 perfect
Dolomite	$CaMg(CO_3)_2$	9.200	2.8 – 2.99	e,o	eu,s	3 perfect
Biotite	$(K,H)_2(Mg,Fe)_2(Al,Fe)_2(SiO_4)_3$	12.296	2.69 – 3.16	p	s,eu	perfect in 1 direction
Muscovite	$K_2O.3Al_2O_3.6SiO_2.2H_2O$	9.428	2.76 – 3.00	p	s,eu	perfect in 1 direction
Mafic minerals						
amphibole (hornblende)	$Ca(Mg,Fe)_3(SiO_2)_4Al_2(Mg,Fe)_2(AlO_3)_2(SiO_3)_2Fe(Mg,Fe)_2(FeO_3)_2(SiO_3)_2$	12.645	3.0 – 3.5	e,o	eu,s,a	2 good, at 56 and 124°
Epidote	$4CaO.3(AlFe)_2O_3.6SiO_2.H_2O$	13.073	3.07 – 3.50	e,o	eu,s,a	1 good, 1 poor, 115° between
Pyroxene (augite)	$CaMg(SiO_3)_2 + (Mg,Fe)(AlFe)_2SiO_6$	11.652	3.2 – 3.6	e,o	eu,s,a	2 good, at 90°
Olivine	$(Fe,Mg)_2SiO_4$	13.556	3.26 – 3.4	e,o	eu,s,a	so poor that rarely seen
Sphene	$CaO.TiO_2.SiO_2$	12.000	3.4 – 3.56	e,o	eu,s,a	
Garnets						
Grossularite	$3CaO.Al_2O_3.3SiO_2$	10.300	3.4 – 3.6	e	eu,s	
Uvarovite	$3CaO.Cr_2O_3.3SiO_2$	10.200	3.418 – 3.81	e	eu,s	
Andradite	$3CaO.Fe_2O_3.3SiO_2$	11.600	3.64 – 3.90	e	eu,s	
Almandite	$Al_2O_3.3FeO.3SiO_2$	11.200	3.688 – 4.33	e	eu,s	
Spessarite	$3MnO.Al_2O_3.3SiO_2$	11.050	4.0 – 4.3	e	eu,s	
Oxide/sulfide minerals						
Zircon	$ZrSiO_4$	14.333	4.02 – 4.86	e,p	eu,s	none
Ilmenite	$FeO.TiO_2$	14.400	4.44 – 4.90	e,o	s,eu,a	none
Magnetite	Fe_3O_4	15.714	4.967 – 5.180	e,o	s,eu,a	none
Hematite	Fe_2O_3	15.200	4.9 – 5.3	p	a	none

Key: o = oblate, p = prolate, e = equant, eu = euhedaral, s = subhedral, a = anhedral
Note: All formulae and estimates of specific gravity are from Hodgman (1948:1248-1265) except for those of the clays, which come from Brady (1974:87) and Hodgman (1948:1689).

scale, the mean atomic number of clays of various types falls somewhere between 7.2 and 10.5. Their specific gravity ranges between approximately 1.8 to 2.6, with most near the 2.6 end (Table 3). Because clay types distribute by their weathering environment and parent material, the mean atomic numbers and specific gravities of clays in a region will usually fall within a much more restricted range. Clays selected for potting will have a yet smaller range. The mean atomic number and specific gravity of clays within a single vessel will usually be almost invariant. In contrast, the mean atomic numbers of common mineral aplastics that might be found in a vessel, or in
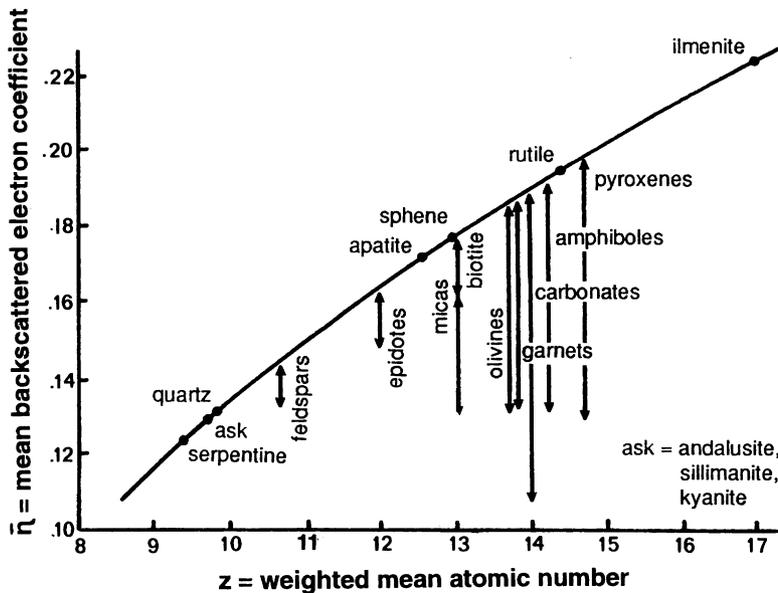
Figure 2. Different minerals have different but overlapping ranges of mean BSE coefficients. The mean BSE coefficient of a mineral is a function of its weighted mean atomic number. Adapted from Hall and Lloyd (1981).

multiple vessels from a site or region, ranges from about 9 to 15. Their specific gravity ranges between approximately 2.5 and 5.3 (Table 3). Thus, the clay matrixes of sherds often can serve as an acceptable as well as convenient "standard" for assessing the XRGLs of rock aplastics.

The potential for particles of different minerals and a set thickness to produce images of different XRGLs is suggested in Table 3. Here, some common rock-forming minerals are ordered by their mean atomic numbers and specific gravities. One finds that orthoclase, plagioclase, and quartz have atomic numbers and specific gravities very similar to clays. Particles of these minerals can be expected to produce x-radiographic images similar in gray level to each other and to the standard clay matrix in which they are embedded. This we find true empirically (see below). In contrast, oxides (e.g., ilmenite, magnetite, hematite, zircon) and sulfides have mean atomic numbers and specific gravities much higher than those of clays. Particles of these minerals can be expected to produce x-radiographic images that are much brighter than those of particles of other minerals and the clay matrix. This, too, we find true empirically (see below). Although all minerals are not distinguishable by their expected XRGL alone,

many more are potentially distinguishable when XRGL is combined with morphological and macrostructural information (Table 2).

The relationship between the XRGL of a rock particle and its mineralogy has a useful analog in back-scattered scanning electron microscopy (BSEM) techniques. BSEM techniques involve the focusing of a beam of electrons on a small portion of a polished, carbon-coated specimen and the detection of the reflected, widely scattered electrons that have energies of greater than about 50 eV. A back-scattered scanning electron (BSE) coefficient is then defined as the ratio of the detected electron current that is back-scattered to the electron current of the incident beam. The mean BSE coefficient of a substance depends ultimately on its weighted mean atomic number (Hall and Lloyd 1981; Lloyd 1987; Robinson 1980). Variation in the composition and the BSE coefficient over a specimen can be displayed as a black-gray-white pixel image similar in looks to an x-radiograph. In geological applications, the image gray level or mean BSE coefficient of a crystal within a polished rock specimen is used, along with its morphology, to identify its mineralogy (Komorowski 1991; Krinsley and Manley 1989; Lloyd 1987; Pye and Kinsley 1984;
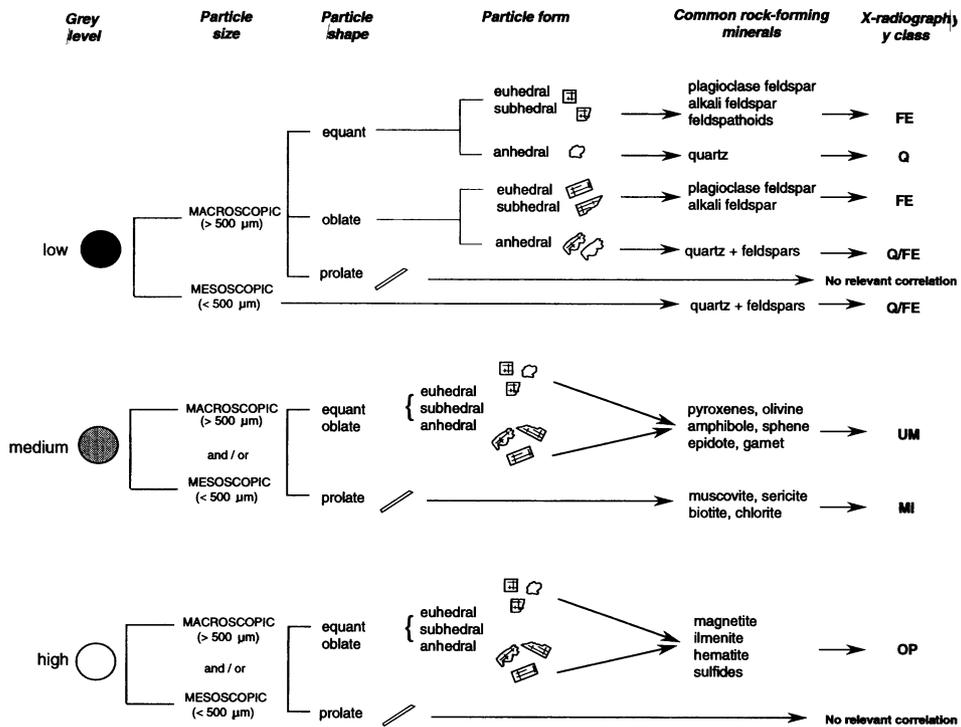
Figure 3. Key for identifying the general kinds of minerals that make up rock aplastics in ceramics from their x-radiographic image.

Robinson and Nickel 1979). In ceramic research, the image gray level or mean BSE coefficient of a rock particle within a polished sherd section can be used, along with its morphology, to identify its mineralogy (Burton 1986).

The relative gray level of a particle's image in an x-radiograph of a ceramic specimen is analogous to the gray level of its image in a display of the specimen's BSE coefficients. In both cases, image brightness is an increasing function of the mean atomic number of the particle, which depends upon its mineralogy. Consequently, it is possible to adapt established BSEM criteria, which identify the mineralogy of a particle by its BSE image gray level or mean BSE coefficient, to the interpretation of a particle's relative gray level in an x-radiograph.

Figure 2 shows the range of mean BSE coefficients of several kinds of minerals, which vary in their mean atomic numbers. Different minerals have different but overlapping ranges of mean BSE coefficients. Analogously, different minerals can be expected to have a similar pattern of different but

overlapping ranges of XRGLs. Some minerals (e.g., quartz, ilmenite) have unique mean BSE coefficients and should have approximately unique XRGLs. Other mineral species that belong to solid solution series or that vary in composition (e.g., micas, olivines, amphiboles, pyroxenes) can have mean BSE coefficients that range more widely and should similarly have more widely ranging XRGLs.

There are two qualifications to the analogy between the XRGL of a rock particle and its mean BSE coefficient. First, the mean BSE coefficient of a specimen is an absolute measure, in the sense that it is not calibrated relative to some material standard. It is the ratio between the detected and emitted electron current for the targeted material, alone. In contradistinction, an XRGL is a relative measure. It is the contrast or difference between a specimen's gray level and the gray level of a standard, such as the clay matrix that surrounds a particle. This contrast varies significantly with the composition and thickness of the chosen standard and many parameters of the selected radiographic technique (Carr and Riddick 1990).

If an aluminum, steel, or lead sheet of set thickness is radiographed with sherds to provide a standard, assessment of the XRGLs of aplastic particles will be consistent across vessels. If the clay paste of vessels is used as the "standard" for defining the XRGL of aplastic particles, variation in the clay's thickness or specific gravity within or among specimens will cause the XRGL of the particles to vary somewhat more widely than their corresponding mean BSE coefficients. Variation in the specific gravity of clays as a function of their porosity might result from differences in their preparation (e.g., levigation vs. raw-clay use) or firing temperature and crystallization. In our work with low-fired Ohio Woodland pottery, neither thickness nor porosity variations were found problematic; differences in particle mineralogy were not obscured. This was true even when comparing specimens at the extremes of variation of Woodland pottery production, which ranged in thickness from 3 to 15 mm and varied noticeably in porosity and strength. The effects of variation in clay (i.e., sherd) thickness were accommodated through exposure adjustments (Carr and Riddick 1990:Figures 11, 12), and the effects of variation in porosity were apparently negligible. Variation in x-radiographic technical parameters affected the XRGLs of rock particles very much more than did variation in clay thickness, clay porosity, and particle mineralogy.

A second qualification to the analogy between the XRGL and mean BSE coefficient of an aplastic particle is that its XRGL depends on its thickness as well as its composition and mean atomic number. This occurs because x-radiography is based on transmitted energy, whereas BSEM is based on reflected energy. Thus, to the extent that particles of the same mineralogy vary in thickness, either within or between specimens, their XRGLs will vary somewhat more widely than their corresponding mean BSE coefficients. Particles of different minerals with similar mean atomic numbers may overlap in their range of XRGLs somewhat more than in their range of BSE coefficients.

Specifically and theoretically, the x-radiographic image density of a particle is equally proportional to its thickness and its linear attenuation coefficient.[2] For two sets of particles of two different minerals to be always distinguishable in their XRGLs, alone, the amount of overlap in the ranges of thickness of the particles of the two sets should be less than the difference in the linear attenuation coefficients of the two minerals. Theoretically, particles of two different minerals should differ in thickness by less than a maximum of 12 fold to be distinguishable by their XRGLs, alone.[3] (These restrictions apply only when the set of thicker particles has the lower linear attenuation coefficient and the thinner set has the higher coefficient, such that the thicknesses and the linear attenuation coefficients of the particles tend to negate each other's effects on the XRGLs of the particles. The restriction is irrelevant when the thicker particles have the higher linear attenuation coefficient and the thinner particles have the lower coefficient.)

Empirically, in our examination of coarse Ohio Woodland pottery with kilovoltages of 30–50 kVp, we found that differences in XRGLs of rock particles due to variation in their thickness became similar in magnitude to differences in their XRGL due to mineralogical variation for only some pairs of mineral species having close mean atomic numbers (see below). This was often true even for particles ranging widely in thickness (e.g., .5 to 5 mm). Also, all differences in particle XRGL due to variation in particle thickness were much smaller than differences due to changing the parameters of the x-radiographic technique (e.g., peak kilovoltage setting, film type).

Given these two qualifications, the mean BSE coefficient response function (Figure 2) can theoretically be used as only an ordinal-scale guide, not a continuous-scale guide, to the x-radiographic interpretation of particle mineralogy. In contrast, the response function can theoretically be used as a continuous scale in BSEM applications to identify some minerals with unique mean BSE coefficients (e.g., quartz, apatite; Figure 2).

In practice, however, identifying the mineralogy of aplastic particles by x-radiography does not differ qualitatively from identifying them by BSEM. An ordinal-scale approach to surveying and interpreting mineralogy is required and used in BSEM practice as well. This is so because the mean atomic numbers and mean BSE coefficients of solid solution series minerals and micas vary

widely (Figure 2), and because such species are common among the rock-forming minerals. Mean BSE coefficients are used as a general guide to mineral identification in the context of crystal morphological and other attributes, just as XRGLs are best used contextually along with other crystal attributes. In BESM research, continuous-scale application of the mean BSE coefficient response function, alone, to identify crystal mineralogy has been useful only when focusing on minerals with unique mean BSE coefficients.

At an operational level, a more significant difference between x-radiographic and BSEM procedures is the range of gray levels over which images of different minerals are spread. In BSEM work, a window of back-scattered electron coefficient levels can be defined and the image gray levels of aplastic particles can be spread from black to white within the window. This maximizes the brightness differences among minerals. In x-radiography, film images of particles have a narrower range of gray levels. In our experience, this made it more difficult to define mineralogical distinctions in x-radiographs. At the same time, we did not use image enhancement procedures analogous to those used in BSEM work to maximize the spread of image gray levels. Such procedures are feasible and would improve x-radiographic studies. Their application deserves further investigation.

In sum, the approximately ordinal-scale relationship between the mean BSE coefficient and the mineralology of a crystal (Figure 2; Hall and Lloyd 1981) can be applied to the relative gray levels of rock particle images in an x-radiograph to help identify their mineralogy. This analogy is productive because both the XRGL and mean BSE coefficient of any substance depend primarily on its mean atomic number.

Key for Identifying Mineralogy

The morphological and structural traits of rock aplastics that are observable in ceramics x-radiographically are fewer in number, different, and sometimes less precise indicators of mineralogy than their petrographically observable analogs (Table 2). Consequently, traditional taxonomic keys of rules by which minerals are identified in geological petrography (e.g., Berry et al. 1983;

Klein and Hurlburt 1985) must be modified when applied to an x-radiograph of a ceramic specimen.

Figure 3 shows one key that we developed for x-radiographic mineral identification through reiterative deduction, induction, and testing. The key is very conservative in the range of particle traits it requires to be observable. It uses only the four most consistently x-radiographically observable particle traits of the seven listed in Table 2. The number and angle of crystal faces and particle internal texture are not used. Also, the number of distinct states required to be observable for each trait is minimal. Only three gray levels and two size classes of particles are used. Finally, the key uses no contextual or associative information (e.g., potential rock sources, associations among minerals as assemblages), which sometimes is used in petrographic identification.

Being conservative in these ways, the key is widely applicable, but distinguishes fewer minerals and mineral families than would be possible in many applications. The key is best characterized as a minimal, foundation key to which more attributes and more detailed attribute states can be added, as the situation permits.

The first and most important level of discrimination made in the key divides rock aplastics qualitatively by their XRGL into three classes. Those minerals that produce dull images that contrast little from the image of their surrounding clay matrix have mean atomic numbers and specific gravities close to those of clays. All of these minerals are felsic: plagioclase and alkali feldspars, feldspathoids, and quartz. Calcite would also fall into this category theoretically but was not among the minerals in the Ohio pottery used to test the key. Those minerals that produce very bright images that contrast most from the image of their surrounding clay matrix have mean atomic numbers and specific gravities much higher than those of clays. Included among these minerals are the oxides (magnetite, ilmenite, hematite, and zircon) and sulfides. The remaining, intermediate range of the XRGL spectrum is produced by a mixture of felsic and mafic minerals having intermediate mean atomic numbers and specific gravities. These include the felsic and mafic micas (muscovite, sericite, biotite, and

chlorite), dolomites, and certain other mafic minerals (e.g., pyroxenes, olivines, amphiboles, sphene, epidote, garnets). Many of these minerals belong to solid solution series that range in their BSE coefficients.

A somewhat finer classification based on XRGL, alone, can be defined if a strict analogy is made between a mineral's mean BSE coefficient on a continuous scale and its XRGL. This approach allows the consistent discrimination of quartz from feldspars, biotite from other micas, and epidotes and sphenes from other mafic minerals (Figure 2). However, the approach does not allow the discrimination of certain mafic minerals that belong to solid solution series, such as olivines, garnets, amphiboles, and pyroxenes.

The second and next most important level of discrimination made by the key distinguishes rock particles with an intermediate XRGL into two classes by size. These are the micas (< 500μm) and a variety of mafic minerals (> 500μm).

Crystal outline shape and form are the remaining characteristics used in the key to divide particles into mineralogical classes. These traits allow the distinction of quartz from feldspars for most macroscopic crystals and strengthen the distinction between micas and mafic minerals based on crystal size. The categories of crystal shape (equant, oblate, prolate) are two-dimensional modifications of the three-dimensional classification of shapes by Zingg (1935), as shown by Pettijohn (1975). The categories of crystal form are based on whether all or some of a crystal's original faces are present (euhedral, subhedral) or none are present (anhedral) (Pettijohn 1975). Euhedral forms cannot be discriminated unequivocally from subhedral forms in an x-radiograph, in contrast to their distinction in a petrographic thin section.[4]

The basic key presented in Figure 3 can be extended with additional attributes and contextual, case-specific information in order to make finer mineralogical distinctions. In favorable weathering and petrological environments, the number and angle of crystal faces and particle internal texture can be used. In our studies of Ohio ceramics, adding these traits allowed us to further distinguish k-spars; other feldspars; sericite; and pyroxene, amphiboles, or pyriboles more generally. A variety of kinds of contextual

information can also be added to the key. These include (1) the correlation of minerals as assemblages, (2) petrological information on the rock sources of the particles, which may suggest the expectable proportions of mineral classes and assemblages, (3) information on the degree of weathering, transport, and/or sorting of the particles, (4) information on consistent mineral alterations, such as the sericite (muscovite) fibrous intergrowths in feldspars, which may systematically distinguish them from quartz, and (5) cultural patterns of selection of tempering materials.

Note that throughout the above, the felsic or mafic nature of a particle is not identifiable directly by x-radiography. Felsic and mafic rocks are usually defined by their light versus dark coloration, which is not visible x-radiographically. Instead, a particle is identified to its more specific mineral or mineral family by other x-radiographically observable traits. This identification then implies its felsic or mafic nature.

Tests of the X-Radiographic Method

The approach to mineral identification introduced here entails fundamental developments of three kinds: (1) industrial and medical x-radiographic techniques have been adapted to the study of ceramics; (2) traditional petrographic principles of mineral identification have been extended to x-radiography; and (3) BSEM approaches to mineral identification have been applied to x-radiography. Because the proposed approach might not work for reasons pertaining to any of these areas of development or their interaction, we constructed tests of it. We asked whether persons trained in geological petrography and BSEM mineral identification could adapt their skills to an x-radiograph and accurately identify rock aplastics in pottery. Our aims were to assess the level of accuracy of the method, to reveal its strengths and limitations, and to define boundary conditions for its appropriate application.

Toward these ends, we made two blind tests of the method. In both, x-radiographic identifications of the mineral species of rock aplastics were compared to petrographic identifications. The studies were made by Komorowski, who is familiar with both BSEM and petrographic methods

Table 4. A Comparison of X-Radiographic and Petrographic Mineral
Identification of Aplastic Particles in Ohio Woodland Sherds.

Particle	Sherd	Optical Petrography of Sherd Thin Sections	X-radiography of Sherd Thick Sections
1-1	2-1	plagioclase (FE) + sericite (MI)	alkali feldspar / plagioclase (FE)
2-2	"	plagioclase (FE) + sericite (MI)	alkali feldspar / plagioclase (FE)
3-3	"	plagioclase (FE) + sericite (MI)	alkali feldspar / plagioclase (FE)
4-6	23-C-07	plagioclase (FE)	alkali feldspar / plagioclase (FE)
5-7	"	plagioclase cluster (FE)	alkali feldspar / plagioclase (FE)
6-8	23-C-32	quartz cluster (Q)	quartz (Q)
7-9	47-D-06	augite cluster + biotite + quartz (UM + MI + Q)	quartz (Q) + mica (MI) or amphibole / pyroxene (UM)
8-10	"	quartz (Q) + biotite inclusion (MI)	alkali feldspar / plagioclase (FE)
9-11	"	quartz cluster (Q)	quartz (Q) + mica (MI)
10-12	"	quartz (Q)	quartz (Q)
11-13	"	biotite (MI) + quartz (Q) + alkali feldspar (FE) + chlorite (MI) + tiny pyroxene (UM)	quartz/alkali feld/plag (Q / FE) + mica (MI) + small opaque (OP)
12-14	"	quartz (Q)	quartz (Q)
13-16	47-D-19	quartz (Q) + alkali feldspar (FE)	quartz/alkali feld/plag (Q / FE)
14-19	47-D-18	alkali feldspar (FE) + amphibole (fibrous) (UM)	alkali feldspar / plagioclase (FE) + sericite (MI)
15-1	11-4	pyroxene (UM) + opaque (OP)	pyroxene / amphibole (UM) + opaques (OP)
16-2	"	pyroxene (UM) + opaque (OP) + plagioclase (FE)	pyroxene / amphibole (UM) + alkali feldspar / plagioclase (FE)
17-3	"	pyroxene (UM) + opaque (OP) + plagioclase (FE)	pyroxene / amphibole (UM) + opaques (OP) + quartz ? (Q)
18-4	"	plagioclase (FE)	alkali feldspar / plagioclase (FE)
19-5	"	pyroxene (UM)	pyroxene / amphibole (UM)
20-6	"	pyroxene (UM) + plagioclase (FE)	pyroxene / amphibole (UM) + opaques (OP) + quartz (Q)
21-7	28-C-42	pyroxene (UM)	opaque (OP) or pyroxene / amphibole (UM)
22-10	40-E-01	quartz cluster (Q)	quartz (Q)
23-11	"	pyroxene (UM) + plagioclase (FE) + opaques (OP) + mica (MI)	pyroxene / amphibole (UM) + quartz / alkali feld / plag (Q / FE)
24-12	"	pyroxene (UM) + plagioclase (FE) + opaques (OP)	pyroxene / amphibole (UM) + + quartz / alkali feld / plag (Q / FE)
25-13	"	pyroxene (UM) + plagioclase (FE) + opaques (OP)	pyroxene / amphibole (UM) + + quartz / alkali feld / plag (Q / FE)
26-14	"	pyroxene (UM) + plagioclase (FE) + opaques (OP)	alkali feld - plag (FE) in pyroxene / amphibole (UM)
27-15	44-2	alkali feldspar (FE)	alkali feldspar / plagioclase (FE)
28-16	"	alkali feldspar (FE) + quartz (Q)	alkali feldspar / plagioclase (FE)
29-17	"	alkali feldspar (FE)	alkali feldspar / plagioclase (FE)
30-18	"	alkali feldspar (FE)	quartz (Q)

Note: Mineral identifications are described as specifically as possible by petrography and x-radiography. Fine-resolution identifications are listed first, followed in parentheses by their more general classification used in the taxonomic key in Figure 3.

(Komorowski 1991). The selected specimens were sherds of utilitarian ceramic jars from archaeological sites in Ohio. The sites date from the Early through Late Woodland period. All of the specimens were tempered with crushed igneous and metamorphic rocks gathered from glacial till and/or outwash. Each specimen was selected by Carr based on the great mineralogical diversity of its aplastics.

The x-radiographs that were available for analysis were good but not optimal. Thus, the tests estimate the accuracy of the x-radiographic approach conservatively. Kodak film Industrex M2 was used, whereas single-coated Industrex R

would have provided better resolution of temper particles under magnification. Also, the x-radiographs were observed with a zoomscope with a yellowish incandescent light, whereas white light would have been preferable.

All observations were made at the magnification of 20×. Approximately one minute was devoted to describing and identifying each aplastic particle in Blind Test 1. Approximately 15 to 20 minutes were spent studying each sherd in Blind Test 2. X-radiographic observations were made by Komorowski without his having any knowledge about the mineralogy of the tempering agents in the specimens, their geologic source, or their archaeological provenience or dates. Corresponding petrographic thin and thick sections were studied by Komorowski only after all x-radiographic work was complete for each test.

The two blind tests differ in the potential limitations of the x-radiographic method that they explore. The first test eliminated the possible problems of interspecimen differences in sherd thickness and of overlap of particle images. The second test admitted these sources of variation.

Blind Test 1

Ten sherds were sectioned 2 mm thick, perpendicular to their wall surfaces, and were x-radiographed. Petrographic thin sections were made from adjacent slices of the sherds. Then, 30 temper particles, which occurred in both the x-radiographs and the thin sections, were assessed for their mineralogy, first x-radiographically and then petrographically (Table 4). The particles consisted of both monomineralic crystals and polymineralic assemblages. Minerals were identified x-radiographically and petrographically as specifically as possible, often beyond the level of distinctions made in the general taxonomic key. This was done by considering information additional to the mineral traits in the key, including crystal cleavage, crystal internal texture, associations among minerals as assemblages, and consistent serecite mineral alterations in feldspars.

The rate of accuracy of x-radiographic identification was calculated using a fourfold contingency table and two ratios of comparison, as shown in the Appendix. X-radiographic and petrographic identifications were compared using the general classes of the taxonomic key. Two equivocal identifications (particles 17, 21) were given half counts as appropriate. Using this procedure, the rate of correct x-radiographic identifications in this blind test is 74 percent and the rate of incorrect x-radiographic identifications is 37 percent. The two percentages do not add to 100 percent because the comparison is asymmetric. The rates err on the side of inaccuracy for the procedural reasons described above.

Blind Test 2

Six whole sherds were x-radiographed in plan view. Petrographic thin sections were then cut from them perpendicular to their wall surfaces. All minerals present in all monomineralic crystals and polymineralic assemblages in the sherds were identified from their x-radiographs (Table 5). All minerals present in the thin sections were then identified petrographically (Table 5). By using whole sherds, the potential problem of intersherd variation in thickness and of overlapping particle images could be assessed. As before, minerals were identified as specifically as possible, using information additional to the mineral traits in the taxonomic key.

The rate of accuracy of x-radiographic identification was calculated using the same fourfold contingency table as above but a different, relevant and analogous pair of ratios of comparison (Appendix). Again, accuracy was measured using the general classes of the taxonomic key. Using this method, the rate of correct x-radiographic identifications in this blind test is 87 percent and the rate of incorrect x-radiographic identifications is 13 percent. The estimated rate of "correct" mineral identifications might be conservatively low and the estimated rate of misidentifications might be conservatively high. Technical reasons for this are explained above and test procedural reasons for this are explained in the Appendix. The rates in Blind Test 2 are better than those in Blind Test 1 because comparison is made between populations of particles rather than individual particles.

Strengths and Limitations of the X–Radiographic Method

The two blind tests suggest that x-radiography can be used to distinguish the minerals and families of

Table 5. A Comparison of X-Radiographic and Petrographic Mineral
Identification of the Collections of Aplastic Particles in Ohio Woodland Sherds.

Sherd	Optical Petrography of Sherd Thin Sections	X-radiography of Whole Sherd
67-D-32	alkali feldspar (> 1 mm) (FE)	alkali feldspar / plagioclase (2–4 mm) (FE)
	plagioclase (FE)	alkali feldspar / plagioclase (2–4 mm) (FE)
Crystals	plagioclase with sericite (FE, MI)	mica (fibrous) (MI)
	pyroxene (0.5 mm) (UM)	amphibole / pyroxene (~ 0.5 mm) (UM)
	hematite (0.25 mm) (OP)	opaques (< 0.5 mm) (OP)
Lithic assem.	alkali feldspar + pyroxene (FE, UM)	quartz / alkali feldspar / plagioclase + sericite (Q/FE, MI)
35-B-38	plagioclase (> 1 mm)	alkali feldspar / plagioclase (~ 1 mm) (FE)
Crystals	quartz (≤ 2 mm) (Q)	quartz (0.5–2.5 mm) (Q)
	biotite (0.5–1 mm) + (MI)	
	amphibole (0.5–1 mm) + (UM)	quartz / alkali feldspar / plagioclase + mica (Q/FE, MI)
Lithic assem.	muscovite (> 1 mm) (MI)	(0.5–1.5 mm)
	plagioclase + biotite + amphibole (FE, MI, UM)	quartz / alkali feldspar / plagioclase + mica (Q/FE, MI)
	(1–1.5 mm)	(0.5–1.5 mm)
	myrmekite (1 mm) (Q, FE)	
35-B-26	quartz (0.5–2 mm) (Q)	quartz (0.5–1.5 mm) (Q)
	alkali feldspar with sericite (FE, MI)	mica (0.5–1 mm) (MI)
Crystals	plagioclase with sericite (0.5–1 mm) (FE,MI)	alkali feldspar / plagioclase (1–1.5 mm) (FE)
	hematite (OP)	opaque minerals (0.5 mm) (OP)
Lithic assem.	plagioclase + quartz + pyroxene (FE, Q, UM)	quartz / alkali feldspar / plagioclase + mica (Q/FE, MI)
24-B-35	alkali feldspar (0.5–1 mm) (FE)	alkali feldspar / plagioclase (3–4 mm) (FE)
Crystals	opaque (0.5–1 mm) (OP)	opaques (< 0.5–1 mm) (OP)
Lithic assem.	perthitic alkali feldspar + opaques (FE, OP)	quartz / alkali feldspar / plagioclase + amphibole / pyroxene + mica + opaques (Q, FE, UM, MI, OP)
23-C-38	alkali feldspar (FE)	quartz / alkali feldspar / plagioclase (1–3 mm) (Q/FE)
		quartz / (1–2 mm) (Q)
Crystals		amphibole / pyroxene (0.5–1.5 mm) (UM)
		opaques (hematite ?) (< 0.5 mm) (OP)
Lithic assem.	pyroxene + plagioclase + chlorite (> 5 mm) (UM, FE, MI)	amphibole / pyroxene + quartz + alkali feldspar / plagioclase + mica (3–8 mm) (UM, Q, FE, MI)
47-D-22	quartz (0.5–1 mm) (Q)	quartz (0.5–1 mm) (Q)
	plagioclase and/or alkali feldspar (0.5–1 mm) (FE)	alkali feldspar / plagioclase (0.5–1 mm) (FE)
Crystals	myrmekite (> 1 mm) (Q/FE)	
	amphibole (< 0.5 mm) (UM)	amphibole / pyroxene (~ 0.5 mm) (UM)
	mica (< 0.5 mm) (MI)	opaques (0.5–1 mm) (OP)
Lithic assem.	quartz + alkali feldspar (Q, FE)	quartz / alkali feldspar / plagioclase + sericite ? (Q/FE, MI)
	quartz + plagioclase (Q, FE)	quartz / alkali feldspar / plagioclase + sericite ? (Q/FE, MI)

Note: Mineral identifications are described as specifically as possible by petrography and x-radiography. Fine-resolution identifications are listed first, followed in parentheses by their more general classification used in the taxonomic key in Figure 3.

minerals listed in Tables 4 and 5, and discussed above for the extended key, with a minimum of nearly 75 to 85 percent accuracy. More specific mineral identifications and/or levels of accuracy can probably be attained in studies that are not experimental, where contextual and associative information, such as geologically known rock sources and assemblages of minerals in the region, are used. Thus, it is clear that persons trained in BSEM and petrography can adapt their skills to x-radiography in order to identify temper mineralogy. It was also apparent to us while working with the x-radiographs that greater accuracy in mineral identification would have been possible if finer-grained film had been used. Finally, high accuracy can also be attained when classifying temper particles into broader mineral families, e.g., into felsic, mafic, and oxide/sulfide mineral families, most simply.

Certain limitations to using x-radiography were also suggested by the tests:

(1) Quartz can be difficult to distinguish systematically from alkali feldspar and plagioclase because the x-radiographic contrast of these minerals from clay is slight, and, thus, diagnostic boundaries and cleavages are sometimes hard to discern. However, fibrous innergrowths of sericite, which occur within alkali feldspar but not quartz, can help to distinguish these minerals, and did so in the Ohio ceramic sample.

(2) The abundance of low XRGL quartz and plagioclase feldspar can sometimes be underestimated relative to the abundance of other minerals with higher XRGLs because of the low gray-level contrast of quartz and plagioclase from clay.

(3) There can be some bias against seeing and correctly identifying micas and feldspars relative to pyroxenes, amphiboles, and oxide and sulfide minerals in an x-radiograph. This bias does not occur in petrography. It results from the frequent orientation of platy mica and feldspar particles parallel to a vessel's wall, in combination with the plan view of them that an x-radiograph of a sherd offers.

(4) Anhedral-formed particles that lack any of their original diagnostic crystal faces are difficult to identify to species based on only their gray level.

(5) When images of aplastic particles overlap completely in a radiograph, the separate particles may sometimes be perceived wrongly to be one rock fragment. As a result, false associations ("assemblages") of minerals may be derived.

(6) It is sometimes difficult to distinguish and identify the separate minerals in polymineral particles, the images of which happen to overlap. In these situations, gray-level contrasts are reduced and grain boundaries can be difficult to see. The consequence of limitations 5 and 6 is that x-radiography works best for sherds that are thin enough or that have a low enough fractional volume of aplastic particles that particle images do not commonly overlap.

(7) Because it is sometimes difficult to distinguish the separate minerals within individual polymineral particles, x-radiography may underestimate the abundance of polymineralic rock fragments relative to monomineralic fragments. Consequently, inferences about the geological origin and transport of the rock aplastics can sometimes be biased.

(8) When a ceramic is tempered with the powder from crushing rocks as well as the rock fragments, the powder's image can create a fog over an x-radiograph. This can make mineral identification more difficult, in the same way that overlap of particle images can.

(9) Microcracks within sherds and uneven radiographic exposure or back lighting can sometimes create the appearance of false structural features within a particle. This illusion can be recognized once the researcher is sensitive to it.

(10) As in petrography, it is difficult to identify the mineralogy of particles less than roughly a half millimeter in diameter.

Limitations 1, 2, 6, and 7 would have been lessened by using finer-grained, single-coated Industrex R film.

Two additional, related limitations were encountered in the case study described below:

(11) Some mafic minerals could not be distinguished from each other, and several kinds of micas could not be sorted, because of the wide overlap in their mean BSE coefficients.

(12) Some biotite and sericite crystals were misidentified as oxide or sulfide minerals because the crystals appeared brighter in the x-radiographs than one would expect from their position on Hall and Lloyd's (1981) mean BSE coefficient response function.

Boundary Conditions for the Appropriate Application of the X-Radiographic Method

The above strengths and limitations to the x-radiographic method of mineral identification imply certain bounds within which its application is most appropriate. First, x-radiography is best suited to surveying the range of common minerals within and among ceramic assemblages; revealing distinct mineralogical contrasts among ceramic assemblages, or ceramic classes within them; and assessing differences in the proportional spectrum of common minerals or mineral families among ceramic assemblages, or ceramic classes within them. Petrography is more appropriate for making fine mineralogical descriptions of ceramic assemblages, classes, and contrasts among them.

Second, when used alone, x-radiography will commonly be found more appropriate for intersite or intercomponent comparisons of ceramics, where differences in the mineralogy of aplastics are often greater, than for comparisons within a component of short duration, where ceramic classes are often more subtly distinguished. When used in conjunction with finer-grained analytical methods (e.g., petrography, electron microscopy, INAA), x-radiography can be used fruitfully in both intersite and intrasite studies (see example, below).

Third, x-radiography is better suited to distinguishing ceramic classes that differ clearly in the presence-absence of, or moderately in the proportions of, certain minerals or mineral families than it is in discriminating classes that differ subtly in their proportions of minerals or mineral families. Qualitative analysis, rather than quantitative "modal" or point-counting analysis (Chayes 1956), may be more appropriate for distinguishing ceramic classes x-radiographically.

In sum, the quantitative and qualitative assessments of the resolution of x-radiography made above, along with considerations of cost and sample integrity, suggest the appropriateness of x-radiography for describing large samples of sherds, each sherd in moderate detail. The niche of x-radiography in ceramic analysis falls between and overlaps with hand-lens and binocular microscopy, on the one hand, and petrography on the other.

Illustration of the Method

An example of the utility of the x-radiographic method is our preliminary study of the rock-tempered pottery from the McGraw site (Prufer 1965), a late Middle Woodland homestead of Hopewell peoples in Ohio. The goal of the study is to clarify and contrast the locations of manufacture of coarse and fine utilitarian wares found at the site. In turn, this information bears on the manner in which Hopewellian households were integrated socioeconomically, and on the nature of local exchange systems.

The chosen application illustrates how x-radiographic analyses of the mineralogy of ceramic tempers can be combined with finer-grained ceramic analyses (e.g., by electron microscopy, INAA, petrography) to corroborate data patterning and deepen inferences. The study is a conservative test of the x-radiographic method because the sherds come from only one site, and are similar in the mineralogical diversity of their temper and manufacturing methods.

The McGraw Site in Culture-Historical Perspectives

The McGraw site is a small, floodplain settlement in the Scioto Valley in south-central Ohio. It possibly served as a gardening homestead for one or a few households (Smith 1992:63), or as a home base from which various, remote subsistence activities were carried out. It was occupied at least twice, as suggested by the minimally bimodal distribution of 11 radiocarbon dates (Carr 1988; Prufer 1965) and the stratification of refuse deposits (James A. Brown, personal communication 1986). It probably was occupied year-round, if functionally analogous to other, more completely studied Hopewell homesteads (Dancey 1991:68).

McGraw is one of many Middle Woodland homesteads that surround the East Bank and High Bank burial mound–earthwork complexes nearby. Together, the homesteads may have comprised a dispersed community that was integrated by kinship (Greber 1979) and trade (Ford 1974), and by funerary and other ceremonies, corporate labor activities, and/or redistributive feasting in one or another of the mound-earthwork centers (Brown 1982; Carr and Maslowski 1995; Seeman 1979;

Smith 1992:201–248). This reconstruction is based on Prufer's (1964, 1965:137, 1975) now generally accepted model of Ohio Hopewell settlement patterns and more recent elaborations of it (Brown 1982; Dancey 1991; Pacheco 1988; Smith 1992:201–248). At a broader scale, multiple mound–earthwork communities in different drainages or portions of drainages may have been organized loosely into groups with some sense of self-identity, as suggested by stylistic analyses (Carr and Maslowski 1995). Persons of different mound-earthwork communities clearly cooperated with each other, which is indicated by artifact trade within Ohio (e.g., Foradas 1989, 1994; Seeman 1979; Struever and Houart 1972; Vickery 1983:84), but also competed, as evidenced by the taking of trophy skulls (Seeman 1988). This regional pattern of interaction is expectable for tribal and simple rank societies (Chagnon 1983; Rosman 1971; Service 1971).

The x-radiographic analysis of McGraw ceramics that is reported here makes a preliminary attempt to address three related questions about Hopewellian household integration and local exchange. Models of Ohio Hopewell interaction posed by Smith (1992), Seeman (1979), Ford (1974), and Braun (Braun and Plog 1982) vary in regard to these three dimensions:

(1) Were households within a community substantially interdependent economically (Braun and Plog 1982, Ford 1974)? Or were they fairly self-sufficient economically, being integrated more fundamentally by rituals within mound-earthwork complexes, and by the ceremonial gift giving and disposition of valued Hopewell Interaction Sphere items during such rituals (Smith 1992:201–248)?

(2) Was the social integration of households within a community and alliances between communities facilitated by frequent "utilitarian exchange" of common goods, in addition to the "valuables exchange" of finer goods and rarer, symbolic Hopewell Interaction Sphere items (Bohannan 1955)? Seeman (1979) has argued, from archaeological and ethnographic data, that Hopewell mortuary ceremonies included ceremonial feasts that involved the pooling and consumption of very significant quantities of food and the exchange of goods by the households

within a community on a frequent, regular basis. In contrast, more recent archaeological literature has emphasized the sporadic and infrequent exchange and burial of Hopewell Interaction Sphere items (e.g., Brose 1990; Griffin 1965, 1973; Hatch et al. 1990), perhaps implying the infrequency of mound-earthwork mortuary ceremonies and the lack of much exchange of either valued or utilitarian goods in at least the ceremonial sphere.

(3) If utilitarian exchange was important, in what contexts or "spheres of exchange" (Bohannan 1955) did it occur: in sacred mound-earthwork sites, in profane domestic spaces, or both. Ethnographic literature (Malinowski 1961; Trigger 1969; references in Seeman 1979), in combination with ethnological theory (Bohannan 1955), suggest that common goods and valuables can be exchanged in either sacred or profane contexts, in either separate places or side by side.

Our preliminary findings below hint that coarse utilitarian ceramics may have been exchanged in significant quantities among economically interdependent Ohio Hopewellian households. Also, both coarser and finer wares may have sometimes been made in the same location, and possibly were traded together, rather than in the earthwork and domestic spheres separately.

Sample Selection and Analyses

From the approximately 10,000 sherds that make up the McGraw ceramic assemblage, 353 that vary maximally in their surface treatment style, circumference, and wall thickness were selected for study. The sherds come from excavation units B1, C1, C2, D1, and D2, and belong to coarsely made utilitarian jars of the McGraw Cord Marked and McGraw Plain types and to more finely formed and decorated utilitarian jars of the Chillicothe Rocker Stamped and Chillicothe Incised types (Prufer 1965:19–31). The jars were tempered with crushed rocks from glacial tills and valley trains. Both the coarse and fine vessels probably served multiple and similar ranges of utilitarian purposes, like their Illinois Woodland correlates (Braun 1983). The body wall thicknesses and circumferences of the four types overlap considerably, and examples of each type bear carbonized food residues on their interiors from cooking.

The 353 sherds were found to belong to approximately 158 individual vessels using visual and x-radiographic procedures of identification (Carr 1993). Then, 59 sherds, each very probably representing a different vessel, were selected so as to maximize variation in several subtle, potentially isochrestic stylistic traits that might indicate different individual potters or small networks of potters. Thus, the sample was biased toward finding exotic vessels, rather than representative of variation in the assemblage.

Three kinds of studies of the ceramics were made: an electron microprobe analysis of the chemistry of their clay pastes (Yeatts 1990), and x-radiographic and petrographic analyses of the mineralogy of their temper particles. The clay paste chemical analysis served as a framework for and was corroborated by the latter two.

The clay paste chemical analysis revealed six statistically stable groups (A, B1, B2, C, D1, D2) and nine unique outliers (Figure 4; Yeatts 1990:52–53).[5] From what was known of natural clay variation in southern Ohio (Yeatts 1990), these groups were interpreted to represent different natural clay deposits that were used (1) by different households at McGraw at any one time, (2) by different households during different occupations, (3) by the McGraw residents at other settlements in their seasonal "round" to make vessels, which were then brought back to McGraw, and/or (4) by households at other sites to make vessels, which were then exchanged into McGraw.

It is likely that some or all of the nine chemically unique vessels, and others in the smaller of the six chemical groups, were manufactured at sites distant from McGraw and then exchanged into McGraw. This is suggested by the fact that all of the paste chemical variability in the sample of 59 vessels could be encompassed by known chemical variability in natural clay deposits only when considering deposits as far as 25 km from the McGraw site.[6] More particularly, some of the vessels were made of clays probably found in different Hopewellian communities associated with different mound-earthwork complexes than McGraw's. A catchment with a 25-km radius includes the well-known earthworks of Harness, High Banks, Chillicothe, Hopeton, Mound City, Cedar Banks, Dunlap, Hopewell, Frankfort,

Spruce Hill, and Baum, among others, in the valleys of the Scioto River, Paint Creek, the North Fork of Paint Creek, and Deer Creek. Finally, the chemical outliers and smaller chemical groups each constitute a very significant percentage of the sample, implying a significant but unquantifiable rate of importation of vessels into McGraw. Thus, Hopewellian households appear to have been interlinked through utilitarian ceramic exchange and may have been economically interdependent.

The clay chemical study also revealed that both coarse and fine vessels were made of the same or very similar clays; vessels of both styles fell in each of five of the six paste chemistry groups (Yeatts 1990:64–68). This pattern implies that both course and fine wares were manufactured at McGraw. It also suggests that both wares may have been manufactured together at other distant sites as well, and that perhaps both wares were exchanged together into McGraw, given the clay chemical variability of the ceramics relative to natural clay variation.

X-radiographic and petrographic analyses of the mineralogy of the rock temper in 33 of the 59 McGraw vessels were made next to corroborate the patterns found in clay paste chemistry and to extend the inferences drawn. The 33 sherds represent each of the six paste chemistry groups and seven of the nine outliers (Figure 4). For the x-radiographic analysis, each sherd was described for the minerals, families of minerals, and mineral assemblages that constitute its temper (Figure 4). The category of "quartz or feldspar" crystals (Q/FE) was not used in the analysis because it lumps uncertain identifications. The category "quartz or feldspar assemblages" was not used because it is almost always absent from the sherds.

First, the credibility of the clay chemistry groups and the accuracy of the x-radiographic method were indirectly evaluated by determining the degree of correspondence of the chemistry and mineralogy data. For each clay chemistry group and each mineralogical attribute, the percentage of sherds in the group that have the same mineralogical attribute state typifying the group on a presence-absence scale was calculated. The percentages obtained for all nine mineralogical traits were then averaged for each group, providing a mean measure of each group's internal mineralogical

ABUNDANCE
■ > 10 %
■ 1- 10 %
▪ < 1 %

GRAIN SIZE
1 < 0.5 mm
2 0.5 - 2 mm
3 2 - 5 mm
4 > 5 mm

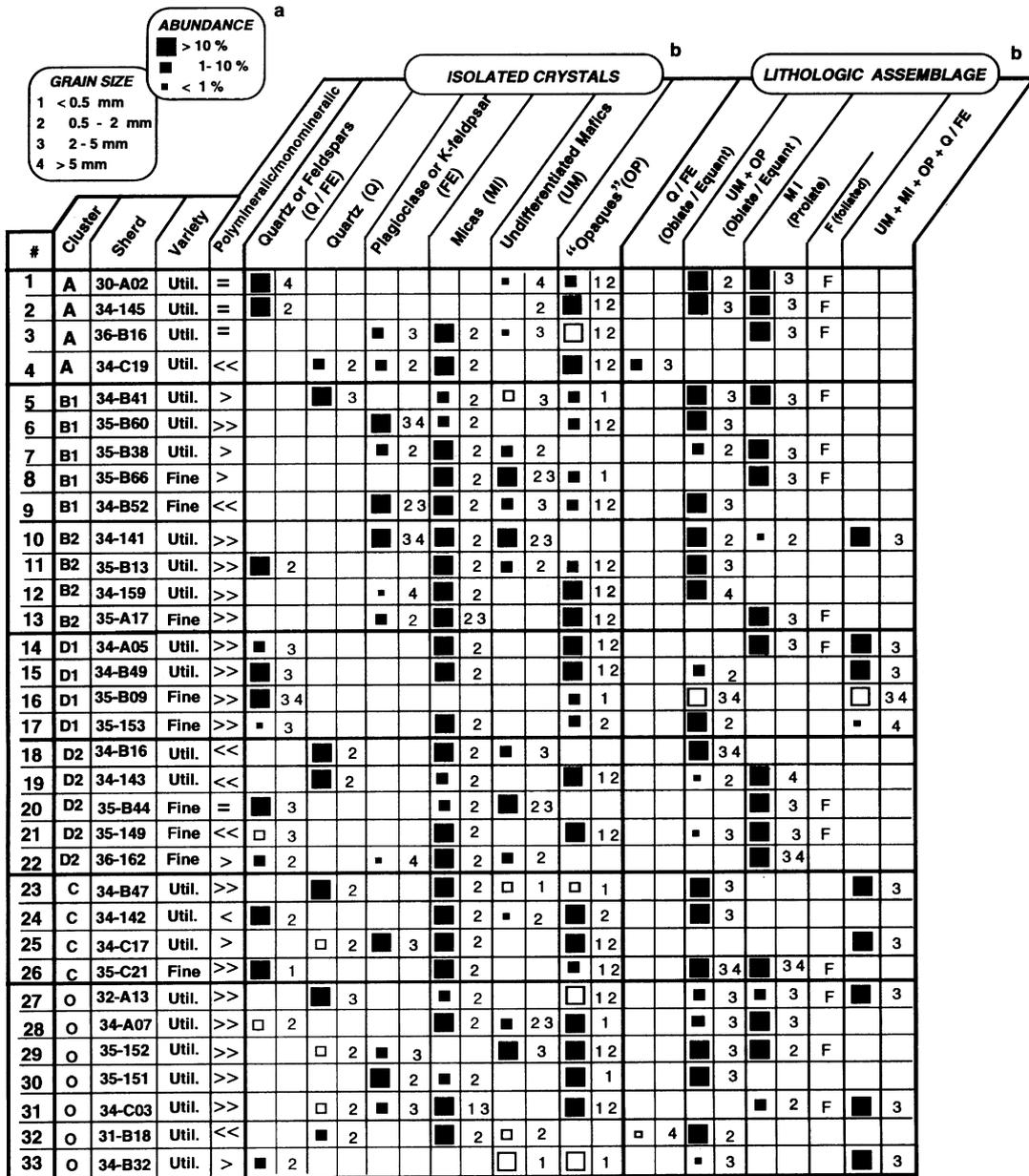| #	Cluster	Sherd	Variety	Grain Size	Polymineralic/monomineralic	Quartz or Feldspars (Q/FE)	Quartz (Q)	Plagioclase or K-feldspar (FE)	Micas (MI)	Undifferentiated Mafics (UM)	"Opaques" (OP)	Q/FE (Oblate/Equant)	UM + OP (Oblate/Equant)	MI (Prolate)	F (foliated)	UM + MI + OP + Q/FE
1	A	30-A02	Util.	=	■ 4					▪ 4	■ 12	■ 2		■ 3	F	
2	A	34-145	Util.	=	■ 2					2	■ 12	■ 3		■ 3	F	
3	A	36-B16	Util.	=				▪ 3	■ 2	· 3	□ 12			■ 3	F	
4	A	34-C19	Util.	<<			▪ 2	▪ 2	■ 2		■ 12	▪ 3				
5	B1	34-B41	Util.	>			■ 3		▪ 2	□ 3	■ 1	■ 3		■ 3	F	
6	B1	35-B60	Util.	>>				■ 34	▪ 2		▪ 12	■ 3				
7	B1	35-B38	Util.	>				▪ 2	■ 2	▪ 2		▪ 2		■ 3	F	
8	B1	35-B66	Fine	>					■ 2	■ 23	▪ 1			■ 3	F	
9	B1	34-B52	Fine	<<				■ 23	■ 2	▪ 3	▪ 12	■ 3				
10	B2	34-141	Util.	>>				■ 34	■ 2	■ 23		■ 2		▪ 2		■ 3
11	B2	35-B13	Util.	>>	■ 2				■ 2	▪ 2	■ 12	■ 3				
12	B2	34-159	Util.	>>				· 4	■ 2		■ 12	■ 4				
13	B2	35-A17	Fine	>>				▪ 2	■ 23		■ 12			■ 3	F	
14	D1	34-A05	Util.	>>	▪ 3				■ 2		■ 12			■ 3	F	■ 3
15	D1	34-B49	Util.	>>	■ 3				■ 2		■ 12	▪ 2				■ 3
16	D1	35-B09	Fine	>>	■ 34					▪ 1		□ 34				□ 34
17	D1	35-153	Fine	>>	· 3				■ 2	▪ 2		■ 2				· 4
18	D2	34-B16	Util.	<<			■ 2		■ 2	▪ 3		■ 34				
19	D2	34-143	Util.	<<			■ 2		▪ 2	■ 2	■ 12	· 2		■ 4		
20	D2	35-B44	Fine	=	■ 3				▪ 2	■ 23				■ 3	F	
21	D2	35-149	Fine	<<	□ 3				■ 2		■ 12	▪ 3		■ 3	F	
22	D2	36-162	Fine	>	▪ 2			· 4	■ 2	▪ 2				■ 34		
23	C	34-B47	Util.	>>			■ 2		■ 2	□ 1	□ 1	■ 3				■ 3
24	C	34-142	Util.	<	■ 2				■ 2	· 2	■ 2	■ 3				
25	C	34-C17	Util.	>			□ 2	■ 3	■ 2		■ 12					■ 3
26	C	35-C21	Fine	>>	■ 1				■ 2		▪ 12	■ 34		■ 34	F	
27	O	32-A13	Util.	>>			■ 3		▪ 2		□ 12	▪ 3		■ 3	F	■ 3
28	O	34-A07	Util.	>>	□ 2				■ 2	▪ 23	■ 1	▪ 3		■ 3		
29	O	35-152	Util.	>>			□ 2	▪ 3		■ 3	■ 12	■ 3		■ 2	F	
30	O	35-151	Util.	>>				■ 2	▪ 2		■ 1	■ 3				
31	O	34-C03	Util.	>>			□ 2	▪ 3	■ 13		■ 12			▪ 2	F	■ 3
32	O	31-B18	Util.	<<			▪ 2		■ 2	□ 2			□ 4	■ 2		
33	O	34-B32	Util.	>	▪ 2						□ 1	□ 1		▪ 3		■ 3

Figure 4. Mineralogical traits of the aplastic particles in sherds from the McGraw Site, Ohio. (a) Open squares denote identifications that are uncertain because of an uncharacteristic combination of x-radiographic gray level and particle shape or form. (b) Mineral identifications are the general families of minerals used in the key in Figure 3. Lithological assemblage refers to groups of crystals that are discernible from each other and the matrix yet form a distinct particle.

consistency. The average mineralogical consistency of the groups ranged from 78 to 94 percent of the sherds per group for the coarse wares and 81 to 88 percent for the fine wares. These correspondences of the paste chemical and temper mineralogical data help corroborate the chemical grouping of sherds. The correspondences also imply that average rates of error in the x-radiographic identification of the mineral traits used, on a presence-absence scale, are no greater than 6 to 22 percent
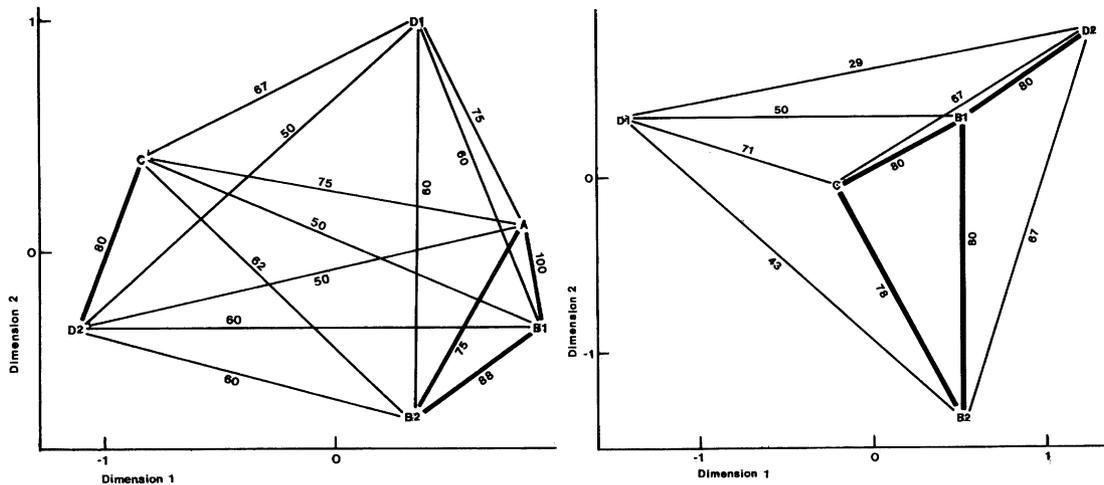
Figure 5. Similarity of clay chemistry groups of (left) coarse-ware sherds to each other and (right) fine-ware sherds to each other, measured by the percentage of typical temper traits that groups share on a presence-absence basis compared to the number available for comparison. Nine traits were available for comparison in most instances. Less than nine traits were available when one or both groups had an even number of sherds with the trait present or absent and its "typical" state was not clear. Bold lines are relationships that are significantly close compared to the minimum level of internal consistency of the groups in their temper traits. The configurations were scaled using SYSTAT's multidimensional scaling routine with a linear objective function and a Minkowski constant of 2. Some "significantly close" clay chemistry groups appear farther apart than their similarity coefficients would suggest, as a result of the data's reduction to two dimensions. For the coarse-ware and fine-ware sherds, Kruskal Stress 1 values are .1170 and .0513, respectively. The proportion of variance in the original data encompassed by the configurations are 86.1 percent and 98.3 percent, respectively.

for the coarse wares and 12 to 19 percent for the fine wares. The errors are probably considerably less, because these percentages combine temper mineralogical variation in each clay chemistry group with observation error.

Petrographic identifications of the mineralogy of temper particles in one-third of the 33 sherds were then made to check for any systematic biases in the x-radiographic identifications. Limitations 1, 12, and 13 (described above) were the most common causes of identification errors. These also had the effect of subduing distinctions among sherd groups defined by their temper traits (below).

Next, we assessed from the x-radiographic data whether the ceramics at McGraw had been tempered with rocks from mineralogically distinct glacial tills and valley trains, with implications regarding vessel exchange. The similarities of each of the six clay chemistry groups of sherds to each other in their temper mineralogy were calculated (Figure 5). Similarity was measured by the percentage of nine typical traits that two groups share on a presence-absence basis. Course and fine wares were evaluated separately. Pairs of

groups were defined as significantly alike when their similarity was near or above the lowest-found level of internal consistency of the groups in their temper traits (78 percent for the coarse wares and 81 percent for the fine wares). In a like manner, the seven coarse-ware sherds that are outliers in their clay chemistry were evaluated for the similarity of their mineralogical compositions to those typical of each of the clay chemistry groups of coarse-ware sherds.

Analyzed in this way, three sets of clay chemistry groups of coarse-ware sherds (B1-B2-A, C-D2, and D1) and two or three sets of clay chemistry groups of fine-ware sherds (B1-B2-C, perhaps D2 as distinct from the former, and D1) were defined as significantly homogeneous internally and different from each other in their temper mineralogy. Also, two of the coarse-ware sherds that are chemical outliers (nos. 29, 31) were found to be unique in their temper traits. The remaining five outliers, despite their chemical distinctiveness, were found to be significantly similar in their temper mineralogy to one or two of the clay chemistry groups of coarse wares (B2, D2, and

perhaps A and D1). In all, seven or eight sets of sherds that are internally homogeneous and externally distinct in their temper mineralogy were defined; three or four of these span multiple clay chemistry groups and are internally diverse in their clay chemistry.

Each of the three or four sets of sherds that is homogeneous in its temper mineralogy yet variable in its clay chemistry can be interpreted most easily as reflecting lithological uniformity over a geographic area greater than areas of natural clay uniformity. Specifically, each set probably represents vessels tempered with rocks derived from a different glacial valley train or till deposit, which in turn spans many natural clay deposits. The surface clays of Ohio are known to differ very significantly and much more locally in their chemistry within broader areas of glacial train and till consistency (Yeatts 1990:68–84; James B. Stoltman and James A. Brown, personal communications 1992, 1994). This local clay diversity probably results from the differential reduction and sorting of rock assemblages during their stream transport and from differential weathering. The remaining three or four sherd sets, which each correlate with only one clay chemistry group, also may reflect different valley trains and tills, because these sets are as distinctive in their temper mineralogy as those spanning multiple clay chemistry groups.

Some of the types of glacial trains and tills represented by the seven or eight distinct sherd sets are probably located in different drainages or sections of drainages, at significant distances from McGraw, and imply vessel exchange. Glacial trains in the different major river valleys of south-central Ohio probably vary somewhat from each other, mineralogically, because their rocks are derived from the action of different glacial sheet lobes, which gathered materials from somewhat different areas of the Canadian Shield. Mineralogy also probably varies within each major river valley, among sections fed by different secondary streams that cut through different tills (Goldthwait et al. 1961).

Other types of glacial trains and tills represented by the seven or eight sherd sets probably occur in the immediate vicinity of McGraw and may have been used by the McGraw residents them-

selves or by members of their community. Several geomorphologically distinct sources of temper are located, conveniently to inconveniently, within 6 km around McGraw.[7] The glacial geology around McGraw is atypically complex.

That some of the types of glacial trains and tills used to temper the McGraw ceramics came from afar, implying vessel exchange, can be inferred from the minimum 25 km. radius of the catchment within which the clays of those vessels were probably derived. This catchment includes several different drainages having glacial deposits that likely vary mineralogically (see above). Moreover, had all or most of the paste and temper sources used for the McGraw ceramics been local, one would expect a random or poorly structured combination of clay and temper types in the vessels. Instead, analysis revealed that the clay chemistry groups systematically correlate with or are nested within the temper-homogenous groups. The large catchment from which clays for the McGraw vessels came also negates the possibility that the several temper sets solely reflect vessels made by separate occupants of McGraw at various times, who preferred different local clay and rock sources.

Implications and Discussion

The most parsimonious explanation of the distinct clusters of McGraw sherds by their temper mineralogy and clay chemistry, as well as the systematic, nested and correlated relationship between these two dimensions of variation, is that a significant proportion of the vessels found at McGraw were exchanged into the site from other households. It appears that some of these households were located far enough from McGraw to have been included in mound-earthwork communities different from McGraw's. These interpretations agree with the results of other preliminary sourcing analyses of Ohio Middle Woodland ceramics (Carr 1992; Elam et al. 1992).[8] Variation in local clay and temper resources around McGraw, their variable use by different McGraw households at one or different times, and/or the accumulation at McGraw of pottery made elsewhere by the McGraw residents during their seasonal round also may account for some of the observed data patterning.

The inferred geographic scale and significant amount of vessel exchange suggest that Ohio Hopewellian households may not have been as self-sufficient, economically, as Smith (1992:201–248) concluded from less sensitive kinds of archaeological data. The McGraw ceramic data also hint that some coarse and fine wares, which were made of similar clays and tempers, may have been manufactured together, at McGraw and other distant sites, and may have been exchanged together from other sites into McGraw. If the finer wares can be interpreted as more valuable because they are less common and because they were used in both mortuary and domestic contexts, while the coarser wares are interpreted as common goods because they are frequent and were used largely in domestic contexts, then the data hint that utilitarian and valuables exchange may have occurred hand-in-hand among households and/or communities in the same context. This context of exchange could have been either domestic sites or mound-earthwork sites. In either case, one need not assume that valued Hopewell items and more common goods were necessarily exchanged respectively in separate, sacred versus profane, spheres.

These implications of the McGraw ceramic analyses should be seen as tentative hypotheses for future studies of local exchange and household integration among the Ohio Hopewell. Study of a larger sample of vessels from a greater number of domestic sites, and fieldwork on the likely geological sources of rock assemblages within vessels, would be worthwhile endeavors. Finally, the analyses presented here clearly show the utility of x-radiography in identifying the mineralogy of rock temper, in corroborating compositional information obtained with other methods, and in extending the inferences drawn.

Conclusion

The x-radiographic method developed and tested here is an essential tool for contemporary archaeology. When research aims at resolving social and ecological processes at a regional level among ceramic-producing societies, and on a quantitative rather than qualitative scale, it is helpful to have a cost-effective strategy for identifying the temper mineralogy of large ceramic samples from multiple assemblages. X-radiography combined with optical petrography offers such a strategy. X-radiography allows the survey and description of large ceramic samples in moderate detail and with economy, in preparation for or in conjunction with more fine-grained, sample-focused, and expensive petrographic work. X-radiography also allows the study of a large and representative volume of a vessel and is nondestructive. X-radiography is best suited to investigating contrasts among multiple, diverse ceramic assemblages regionally or among diverse wares within a site. Problems in ceramic engineering, function, chronology, typology, and trade, which rely on the mineralogical identification of temper, can each be addressed using x-radiography.

References Cited

Bohannan, P.
  1955 Some Principles of Exchange and Investment among the Tiv. *American Anthropologist* 57:60–70.
Berry, L. G., B. Mason, and R. V. Dietrich
  1983 *Mineralogy.* 2nd ed. Freeman, San Francisco.
Bimson, M.
  1969 The Examination of Ceramics by X-Ray Powder Diffraction. *Studies in Conservation* 14:85–89.
Bishop, R. L., R. L. Rands, and G. R. Holley
  1982 Ceramic Compositional Analysis in Archaeological Perspective. *Advances in Archaeological Method and Theory* 5:275–330.

Brady, Nyle C.
1974 *The Nature and Properties of Soils.* 8th ed. MacMillan, New York.

Braun, D. P.
1983 Pots as Tools. In *Archaeological Hammers and Theories,* edited by J. Moore and A. S. Keene, pp. 107–134. Academic Press, New York.
1987 Coevolution of Sedentism, Pottery Technology, and Horticulture in the Central Midwest, 200 B.C.–A.D. 600. In *Emergent Horticultural Economies of the Eastern Woodlands,* edited by W. F. Keegan, pp. 153–181. *Occasional Papers* No. 7. Center for Archaeological Investigations, Southern Illinois University, Carbondale.

Braun, D. P., and S. Plog
1982 Evolution of "Tribal" Social Networks: Theory and Prehistoric North American Evidence. *American Antiquity* 47:504–525.

Bronitsky, G.
1986 Experiments in Ceramic Technology: The Effects of Various Tempering Materials on Impact and Thermal-Shock Resistance. *American Antiquity* 51:73–89.

Brose, David S.
1990 A Model of Exchange Values for the Eastern Woodlands. *Mid-Continental Journal of Archaeology* 15:100–136.

Brown, James A.
1982 Mound City and the Vacant Ceremonial Center. Paper presented at the 47th Annual Meeting of the Society for American Archaeology, Minneapolis.
1984 Overview of the Archaeological Investigations of the Mound City Group National Monument. Manuscript on file, National Park Service, Midwestern Archaeological Center, Lincoln, Nebraska.

Burton, J.
1986 *Selected Petrologic Applications of Backscattered Electron Imaging.* Unpublished Ph.D. dissertation, Department of Geology, Arizona State University, Tempe.

Carneiro, R.
1972 From Autonomous Village to the State: A Numerical Estimation. In *Population Growth: Anthropological Implications,* edited by B. Spooner, pp. 64–77. MIT Press, Cambridge, Massachusetts.

Carr, C.
1988 Ohio Woodland AMS and Beta Radiocarbon Dates. Manuscript on file, Department of Archaeology, Ohio Historical Center, Columbus.
1990 Advances in Ceramic Radiography and Analysis: Applications and Potentials. *Journal of Archaeological Science* 17:13–34.
1992 Modeling the Evolution of Alliance Strategies as Systems Regulators in Egalitarian Societies. In *Grants Completed; Biennial Report of the Wenner-Gren Foundation for Anthropological Research.* Wenner-Gren Foundation, New York.
1993 Identifying Individual Vessels with X-Radiography. *American Antiquity* 53:96–117.

Carr, C., and R. Maslowski
1995 Cordage and Fabrics: Relating Form, Technology, and Social Process. In *Style, Society, and Person,* edited by C. Carr and J. Neitzel, pp. 297–343. Plenum, New York.

Carr, C., and E. B. Riddick
1990 Advances in Ceramic Radiography and Analysis: Laboratory Methods. *Journal of Archaeological Science* 17:35–66.

Carr, C., and D. W. G. Sears
1985 Toward an Analysis of the Exchange of Meteoritic Iron in the Middle Woodland. *Southeastern Archaeology* 4:79–92.

Chagnon, N. A.
1983 *Yanomamö: The Fierce People.* Holt, Rinehart, and Winston, New York.

Chayes, F.
1956 *Petrographic Modal Analysis.* John Wiley and Sons, New York.

Dancey, W. S.
1991 A Middle Woodland Settlement in Central Ohio: A Preliminary Report on the Murphy Site (33LI212). *Pennsylvania Archaeologist* 61(2):37–72.

Eastman Kodak Company
1980 *Radiography in Modern Industry.* Eastman Kodak, Rochester, New York.

Elam, J. M., C. Carr, M. D. Glascock, and H. Neff
1992 Ultrasonic Disaggregation and INAA of Textural Fractions of Tucson Basin and Ohio Valley Ceramics. In *Chemical Characterization of Ceramic Pastes in Archaeology,* edited by H. Neff, pp. 93–112. Prehistory Press, Madison, Wisconsin.

Ford, R. I.
1974 Northeastern Archaeology: Past and Future Directions. *Annual Review of Anthropology* 3:385–414.

Foradas, J. G.
1989 Sourcing of Flint Using Normative Mineral Compositions and the Scanning Electron Microprobe: An Experimental Study Using Flint Ridge Flint. Paper presented at the 54th Annual Meeting of the Society for American Archaeology, Atlanta, Georgia.
1994 *Chert Acquisition for Ceremonial Bladelet Manufacture at Three Scioto Hopewell Sites.* Ph.D. dissertation, Department of Anthropology, Ohio State University, Columbus.

Freestone, I., C. Johns, and T. Potter (editors)
1982 *Current Research in Ceramics: Thin Section Studies.* Occasional Paper No. 32. British Museum, London.

Garrett, E. M.
1986 A Petrographic Analysis of Black Mesa Ceramics. In *Spatial Organization and Trade,* edited by S. Plog, pp. 114–142. Southern Illinois University Press, Carbondale.

Goldthwait, R. P., G. W. White, and J. L. Forsyth
1961 *Miscellaneous Geological Investigations Map I-316.* Ohio Department of Natural Resources, Division of Water and Division of Geological Survey, Columbus.

Greber, N.
1979 Variations in Social Structure of Ohio Hopewell Peoples. *Mid-Continental Journal of Archaeology* 4(1):35–78.

Griffin, J. B.
1965 Hopewell and the Dark Black Glass. *Michigan Archaeologist* 11:115–155.
1973 Hopewell Non-exchange of Obsidian. Paper presented at the Northwestern University Archaeological Research Program Lecture Series, Archaeology and the Natural Sciences. Kampsville, Illinois.

Hall, M. G., and G. E. Lloyd
1981 The SEM Examination of Geological Samples with a Semiconductor Back-Scattered Electron Detector. *American Mineralogist* 66:362–368.

Halmshaw, R.
1982 *Industrial Radiography*. Applied Science Publishers, London.

Hatch, J. W., J. W. Michels, C. M. Stevenson, B. E. Scheetz, and R. A. Greidel
1990 Hopewell Obsidian Studies: Behavioral Implications of Recent Sourcing and Dating Research. *American Antiquity* 55:461–479.

Hodgman, C. D. (editor)
1948 *Handbook of Chemistry and Physics*. Chemical Rubber Company, Cleveland.

Isphording, W. C.
1974 Combined Thermal and X-Ray Diffraction Techniques for Identification of Ceramic Ware Temper and Paste Minerals. *American Antiquity* 39:477–483.

Klein, C., and C. S. Hurlburt, Jr.
1985 *Manual of Mineralogy* (after James D. Dana), 20th ed. John Wiley and Sons, San Francisco.

Komorowski, J.-C.
1991 *Scanning Electron Microscopy of Pyroclastic Matter: Eruptions of Mount Vesuvius in A.D. 79 and Mount St. Helens in A.D. 1980*. Unpublished Ph.D. dissertation, Department of Geology, Arizona State University, Tempe.

Krinsley, D. H., and C. R. Manley
1989 Backscattered Electron Microscopy as an Advanced Technique in Petrography. *Journal of Geological Education* 37:202–209.

Lloyd, G. E.
1987 Atomic Number and Crystallographic Contrast Images with the SEM: A Review of Backscatter Electron Techniques. *Mineralogical Magazine* 51:3–19.

Malinowski, B.
1961 *Argonauts of the Western Pacific*. E. P. Dutton, New York.

Pacheco, P.
1988 Ohio Middle Woodland Settlement Variability in the Upper Licking River Drainage. J*ournal of the Steward Anthropological Society* 18:87–117.

Pettijohn, F. J.
1975 *Sedimentary Rocks*. 3rd ed. Harper and Row, New York.

Plog, F. T.
1974 *The Study of Prehistoric Change*. Academic Press, New York.

Porter, J. W.
1963 *Bluff Pottery Analysis—Thin Section Experiment 2: Analysis of Bluff Pottery from the Mitchell Site, Madison County, Illinois*. Research Report No. 4. Lithic Laboratory, Southern Illinois University Museum, Carbondale.

Prufer, O.
1964 The Hopewell Cult. *Scientific American* 211:90–102.
1965 The McGraw Site: A Study in Hopewellian Dynamics. *Cleveland Museum of Natural History Scientific Publications* 4(1):1–144.
1975 The Scioto Valley Archaeological Survey. In *Studies in Ohio Archaeology*, edited by O. Prufer and D. McKenzie, pp. 267–328. Kent State University Press, Kent, Ohio.

Pye, K., and D. H. Krinsley
1984 Petrographic Examination of Sedimentary Rocks in the SEM Using Backscattered Electron Detectors. *Journal of Sedimentary Petrology* 54:877–888.

Robinson, V. N. E.
1980 Imaging with Backscattered Electrons in a Scanning Electron Microscope. *Scanning* 3:15–26.

Robinson, B. W., and E. H. Nickel
1979 A Useful New Technique for Mineralogy: The Backscattered Electron/Low Vacuum Mode of the SEM Operation. *American Mineralogist* 64:1322–1328.

Rosman, A., and P. Rubel
1971 *Feasting with Mine Enemy*. Columbia University Press, New York.

Rye, O. S.
1981 *Pottery Technology*. Taraxacum, Washington, D.C.

Seeman, M. F.
1979 *The Hopewell Interaction Sphere: The Evidence for Inter-regional Trade and Structural Complexity*. Prehistoric Research Series Vol. 5, No.2. Indiana Historical Society, Indianapolis.
1988 Ohio Hopewell Trophy-Skull Artifacts as Evidence for Competition in Middle Woodland Societies Circa 50 B.C.–A.D. 350. *American Antiquity* 53:565–577.

Service, E. R.
1971 *Primitive Social Organization*. Random House, New York.

Shepard, A. O.
1956 *Ceramics for the Archaeologist*. Carnegie Institution of Washington, Washington, D.C.
1976 *Ceramics for the Archaeologist*. Carnegie Institution of Washington, Washington, D.C.

Simon, A.
1988 *Integrated Ceramic Analysis: An Investigation of Intersite Relationships in Central Arizona*. Unpublished Ph.D. dissertation, Department of Anthropology, Arizona State University, Tempe.

Smith, B.
1992 *Rivers of Change*. Smithsonian Institution Press, Washington, D.C.

Stoltman, J. B.
1989 A Quantitative Approach to the Petrographic Analysis of Ceramic Thin Sections. *American Antiquity* 54:147–160.
1991 Ceramic Petrography as a Technique for Documenting Cultural Interaction: An Example from the Upper Mississippi Valley. *American Antiquity* 56:103–120.

Stout, W., Ver Steeg, K., and G. F. Lamb
1943 Geology of Water in Ohio. *Bulletin 44*. Ohio Division of Geological Survey, Columbus.

Struever, S., and G. Houart
1972 An Analysis of the Hopewell Interaction Sphere. In *Social Exchange and Interaction*, edited by E. Wilmsen, pp. 47–80. Anthropological Paper No. 46. Museum of Anthropology, University of Michigan, Ann Arbor.

Tite, M. S., I. C. Freestone, N. D. Meeks, and M. Bimson
1982 The Use of Scanning Electron Microscopy in the Technological Examination of Archaeological Ceramics. In *Archaeological Ceramics*, edited by J. S. Olin and A. D. Franklin. Smithsonian Institution Press, Washington, D. C.

Trigger, B. G.
1969 *The Huron Farmers of the North*. Holt, Rinehart, and Winston, New York.

Ver Steeg, K.
1946 The Teays River. *Ohio Journal of Science* 46:297–307.

Vickery, K. V.
1983 The Flint Sources. In *Recent Excavations at the*

Edwin Harness Mound, by N. Greber, pp. 73–85. Mid-Continental Journal of Archaeology, Special Paper No. 5. Kent State University Press, Kent, Ohio.

Weymouth, J. W.
  1973 X-Ray Diffraction Analysis of Prehistoric Pottery. *American Antiquity* 38:339–344.

Williams, D. F.
  1983 Petrology of Ceramics. In *Petrology of Archaeological Artefacts,* edited by D. R. C. Kempe and A. P. Harvey, pp. 301–329. Cambridge University Press, Cambridge.

Yeatts, M. L.
  1990 *A Chemical Characterization of the Ceramics from the McGraw Site in Ohio with the Electron Microprobe.* Unpublished Master's thesis, Department of Anthropology, Arizona State University, Tempe.

Zingg, T. H.
  1935 Beitrage zur Schotteranalyse. *Mineralogische und Petrographische Mitteilungen Schweizerische* 15:39–140.

Notes

1. When natural silts are common in the paste of vessels, the paste may or may not be an acceptable standard for assessing the image gray level of aplastics, depending on the consistency of the proportion, mineralogy, mean atomic numbers, and specific gravities of the silts among vessels. Powdered-rock additives are likely to vary more than clays in these parameters, and may make the paste of vessels an unacceptable standard.

2. The x-radiographic density, D, of a particle's image decreases as a function of both its thickness and its linear absorption coefficient:

$$\Delta D = .43 \Delta x\, \mu G_D / (1 - I_S / I_D)$$

where ΔD is a small change in x-radiographic film density, Δx is a small change in particle thickness, μ is the particle's linear attenuation coefficient, G_D is the slope of the film's characteristic curve at film density D, I_S is the intensity of the scattered, fog-producing radiation, and I_D is the intensity of the direct, image-forming radiation (Halmshaw 1982:Equation 2.18). As a first approximation, for most pottery vessels, I_D can be considered zero and the denominator can be ignored.

3. At an x-radiographic kilovoltage setting of 30 kVp, where the bulk of the emitted radiation is approximately 15 keV, and assuming coherent x-radiation scatter, one of the densest minerals found as ceramic aplastics, magnetite (Table 3), theoretically has a linear attenuation coefficient approximately 11.9 times that of quartz, one of the least dense minerals found as ceramic aplastics. The linear attenuation coefficients of magnetite and quartz under these conditions are respectively 1365 and 115 cm^{-1}. These numbers are derived using the "mixture rule" (Hubbell 1969:7) to combine elements into minerals, and the total mass attenuation coefficients (μ/ρ) for elements compiled by Hubbell (1969:Tables 3.1–3.23, column 10), where μ is the linear attenuation coefficient of the element and ρ is its density. Thus, for a set of magnetite particles and a set of quartz particles to be consistently distinguished by their XRGLs alone, the quartz particles should be less than 11.9 times thicker than the magnetite particles. Particles of minerals more similar in their linear attenuation coefficients would have to be more similar in

their thicknesses to be distinguishable by their XRGLs alone.

4. In designing the rules of the key for identifying particle mineralogy, some simplifying assumptions have been made that are very widely but not universally applicable. These assumptions reflect the more limited set of structural and textural characteristics that an x-radiograph documents compared to a petrographic thin section. For example, low XRGL, macroscopic, equant, anhedral crystals are defined as quartz. Although it is possible to find equant anhedral alkali or plagioclase feldspars, depending on particle orientation and modification, these minerals are usually more elongated in one direction. Also, because of their good cleavage in two directions, they are typically bounded by at least one original crystal face. In contrast, quartz does not have good cleavage and is typically equidimensionally shaped in stream sediments, unless the source rock has been highly metamorphized and stretched (e.g., gneiss, schist, quartzite).

5. The microprobe was set with a 100X rastering electron beam of 10 nA at an o operating voltage of 15 KeV. The energy dispersive analyzer was mounted at a 40 take-off angle and had a (Si)Li crystal detector with 144 eV resolution. The beam was focused on the clay components of polished and carbon-coated thin sections of the sherds. The area surveyed for each sherd was made up of five points, each 1.0 x .8 mm, dispersed maximally over the section. Each point was analyzed 100 detector-live seconds for the normalized relative proportions by weight of Na, K, Si, Al, Mg, Ca, S, P, Cl, Mn, Cr, Ti, and Fe. The elemental data were screened and transformed in several ways to eliminate procedural errors and then searched for groups of chemically similar sherds. SAS's ALSCAL multidimensional scaling routine was used for dimensional reduction and smoothing of the data. The smoothed data, in the form of scaled stimulus coordinates, were then displayed in a final version using SAS's average-linkage clustering algorithm based on Euclidean distances between the coordinates. See Yeatts (1990) for further details.

6. Variation in the chemistry of natural surface-clay deposits over space was estimated with 35 samples within the Scioto and Paint Creek drainages from Columbus to Portsmouth. Eight of these samples are within 25 km of McGraw and 20 are within 40 km.

7. Rock from both Wisconsin-age outwash in the Scioto Valley and an Illinoisan-age end morraine were available to potters as sources of rock temper within 1 km of McGraw on the same (west) side of the Scioto River. Less conveniently located were Illinoisan-age outwash 1 km away on the opposite (east) side of the Scioto; other Wisconsin-age outwash deposits brought southeast by Paint Creek, 3 km to the west; and Wisconsin-age end morraine and ground morraine deposits 5 and 6 km away, respectively (Goldthwait et al. 1961). Some alluvial gravels of the preglacial Teays River, which drained the Appalachian Plateau from North Carolina northward, may also have been available (Stout et al. 1943:51–106; Ver Steeg 1946; David Brose, personal communication 1994).

   Teays-age alluvium immediately around McGraw apparently is largely covered by Wisconsin-age outwash (Goldthwait et. al 1961), because here the modern Scioto Valley follows the older Teays. Northwest of McGraw, Teays

deposits are buried beneith Wisconsina-age tills (Stout et al. 1943:52). Moreover, gravels and boulders within the Teays alluvial deposits are rare to absent over most of this low-gradient mature stream, and, where present, they lie on or near the bedrock and are overlain by sands and silts (Stout et al. 1943:54–55). Brose (personal communication 1994), however, has observed various rare minerals and metamorphic rocks, which he attributes to the Teays, 10 miles north of McGraw.

8. Preliminary results of an instrumental neutron activation analysis of the clay chemistry of 204 utilitarian pottery vessels from 13 Woodland through Fort Ancient habitation components distributed over southern Ohio (Carr 1992; see also Elam et al. 1992) indicate that the percentage of vessels imported into the Middle Woodland components averaged ca. 13 percent.

Appendix

Method for Calculating the Rate of Accuracy of X-Radiographic Mineral Identifications of Aplastic Particles

Petrographic Identifications	X-Radiographic Identifications	
	Mineral Present in Particle	Mineral Absent in Particle
Mineral present in particle	(A) petrographically identified mineral in particle also identified x-radiographically	(B) petrographically identified mineral in particle erroneously identified x-radiographically
Mineral absent in particle	(C) mineral not identified petrographically in particle erroneously identified x-radiographically	(D) not relevant

Blind Test 1[a]

correct x-radiographic identifications as a percentage of "true" petrographic identifications

$$\frac{A}{A+B} \times 100\% = \frac{39.5}{53.0} = 74\%$$

incorrect x-radiographic identifications as a percentage of "true" petrographic identifications

$$\frac{B+C}{A+B} \times 100\% = \frac{19.5}{53.0} = 37\%$$

Blind Test 2[b]

correct x-radiographic identifications as a percentage of those "true" petrographic identifications sampled in the thin section

$$\frac{A}{A+B} \times 100\% = \frac{20.0}{23.0} = 87\%$$

incorrect x-radiographic identifications as a percentage of those "true" petrographic identifications sampled in the thin section

$$\frac{B}{A+B} \times 100\% = \frac{3.0}{23.0} = 13\%$$

[a]The ratios for Blind Test 1 assume the petrographic identifications in Table 4 to be true and assess the accuracy of the x-radiographic identifications relative to them, i.e., the comparison is "directional" or "asymmetric." The ratios do not compare the "similarity" of the x-radiographic and petrographic identifications to each other in a "bidirectional" and "symmetrical" way, as in a standard similarity coefficient. Specifically, the number of "correct" or "incorrect" x-radiographic identifications in the numerator are compared to the number of "true" petrographic identifications (A + B cells), alone, in the denominator, rather than to a sum of the x-radiographic and petrographic identifications (A + B + C cells).

[b]As in Blind Test 1, the ratios in Blind Test 2 assume only the petrographic identifications to be true and are directional/asymmetric. However, the ratios also reflect the additional condition that the comparison between x-radiographic and petrographic identifications is not made particle by particle. Rather, it is made between the spectra of minerals identified in the populations of aplastic particles within the x-radiographed sherds and thin sections. In this case, lack of correspondence between the x-radiographically identified and petrographically identified lists of minerals in a specimen can derive from either misidentification by the x-radiographic method or the fact that the particles present in the thin section are only a sample of the particles present in the full volume of the corresponding sherd that was x-radiographed. Thus, the ratio estimating the percentage of incorrect x-radiographic identifications considers only the B cell of the four-fold contingency table, not the B + C cells, in its numerator. Another condition of the comparison between the x-radiographic and petrographic mineral identifications that leads to their lack of correspondence is the different directions of viewing of particles. For the thin sections, the view is perpendicular to the sherd wall. For the x-radiographs, the view is parallel to the sherd wall. This difference could not be accommodated quantitatively. Thus, the estimated rate of "correct" mineral identifications could be conservatively low and the estimated rate of misidentifications could be conservatively high.